THE RELATIONSHIP BETWEEN PROTEIN STRUCTURAL CHARACTERISTICS AND TEMPERATURE OPTIMUM FOR ACTIVITY OF THE MERCURIC REDUCTASE FROM TWO SPECIES OF BACTEROIDETES

By

BAHRAM MANAVI

A thesis submitted to the

Graduate School-New Brunswick

Rutgers, The State University of New Jersey

In partial fulfillment of the requirements

For the degree of

Master of Science

Graduate Program in Microbial Biology

Written under the direction of

Professor Tamar Barkay

And approved by

_____

_____

_____

_____

New Brunswick, New Jersey

October 2014

ABSTRACT OF THE THESIS

THE RELATIONSHIP BETWEEN PROTEIN STRUCTURAL CHARACTERISTICS AND TEMPERATURE OPTIMUM FOR ACTIVITY OF THE MERCURIC REDUCTASE FROM TWO SPECIES OF BACTEROIDETES

By

BAHRAM MANAVI

Thesis Director:

Dr. Tamar Barkay

During the past five decades, mercury has gained increased interest due to its toxicity to human and environmental health. Therefore, mercury detoxification, whereby the mercuric reductase (MR), a homodimer of MerA (Figure 3-10), converts Hg^{2+} to Hg^{0}, is an important activity. *merA*, the gene encoding MerA, has been found in diverse Archaea and Bacteria [1], but it is not well known in the *Bacteroidetes*, a large phylum in the bacterial domain that is widely distributed in many environments. The goal of this study was to identify protein structural characteristics that relate to MerA temperature optimum for activity in two species of the phylum *Bacteroidetes*: one a thermophile, *Rhodothermus marinus*, and the other a psychrophile, *Flavobacterium.* sp. SOK62. The standard MerA assay [2] was optimized by adjusting pH, selecting the reducing substrates (NADH/NADPH) and the type and concentration of thiol agent. Using the optimized assay, I found that the optimum temperature for MerA of *R. marinus* was at

65-70˚C (activity range from 30 to 90 ºC) and for the psychrophilic MerA (strain SOK62) was at 50-55 ˚C (range from 10 to 90 ºC). Homology modeling (Figure 3-7) of the psychrophilic and thermophilic MerA (homology to a proteobacterial MerA from *Pseudomonas aeruginosa* PAT) showed that the psychrophile's MerA (SOK62) has more α-helix and less β-sheet secondary structure than the thermophile's MerA (*R. marinus*), which is shown in Table 3-5. MerA of SOK62 has more polar residues and less hydrophobic residues, suggesting adaptation to activity at lower temperatures [3]than MerA of *R. marinus.* In contrast, the psychrophile's MerA has a larger number of aromatic residues than the *R. marinus* enzyme, contradicting the expectation of a lower number of bulky residues in a psychrophilic protein. These experiments test the hypothesis that because MerA originated among thermophiles in geothermal environments [4], the MerA from a psychrophilic bacterium has a thermophilic enzyme activity optimum and structural adaptations facilitating activity at low temperatures. This study contributes to our understanding of the natural history of microbial mercury detoxification.

Acknowledgement

My sincere gratitude and appreciation to my advisor Professor, Dr. Tamar Barkay, whose support with my thesis was endless. During the past years her attitude was always encouraging and helped me to progress in my research. I wish to thank her for patience, guidance and brilliant ideas.

Besides Professor Barkay, it is my pleasure to thank Professor Kahn, whom I owe for his support and advice prior to my admission to the program, since my first attendance in his biochemistry lecture, and for all his help in my research.

I would like to thank my committee members. It is my greatest honor to have Professors Dr. Tamar Barkay, Dr. Peter Kahn, and Dr. Theodore Chase in my defense.

I am very thankful to Drs. Theodore Chase, Peter Kahn, Max Haggblom, and Douglas E. Eveleigh for their good advice and making their laboratory resources available to me.

I am grateful to past and present members of the Barkay lab; Aspa, Riqing, Zach, and Kim for their help and direction to do my research over the past years.

I want to thank Ameya Mashruwala in the Jeff Boyd lab for guiding me on how to break the cells with the French Press, Udonna Ndu and Sarah Janssen in the John Reinfelder Lab for guidance in performing the mercury volatilization assay and also to Chengsheng Zhu for his work with phylogeny analysis of MerA.

It also gives me pleasure to thank the staff at the Department of Biochemistry and Microbiology, Lucy Hsu, Jessie Maguire, Kathy Maguire, Beth Nugent, Eileen Glick, Arleen Nebel, and Peter Anderson for their assistance.

My sincere gratitude to other faculty members in Lipman Hall, Marine and Coastal science, and ENR who have provided much help and assistance; Drs. Jeff Boyd, Yana Bromberg , John Reinfelder, Nathan Yee, Costantino Vetriani, Lee J. Kerkhof, William Ward, and Gerben Zylstra.

Foremost, I would like to extend my deepest gratitude to my family who always believe in me and for their emotional support.

Dedication

To my parents, Mehrdad and Nasrin and my sister Mehrdokht.

Table of Contents

List of Tables

List of Figures

1 Chapter 1: Introduction

The element mercury is located in group 2B (heavy metals) just below cadmium in the periodic table. It is a liquid metal and is widely used in dental amalgams, thermometers, fluorescent lamps, and also exists in nature from oceans to volcanoes (see Figure 1-1). Hg is an earth crust element that is largely released to the environment by the combustion of fossil fuel. It is a toxic element and can be easily converted to its more toxic form, methyl mercury, by anaerobic microorganisms, which exist in anoxic sediments. Therefore, for microbial life to survive mercury toxicity there must be a system to detoxify, *e.g.*, the *mer* operon system.

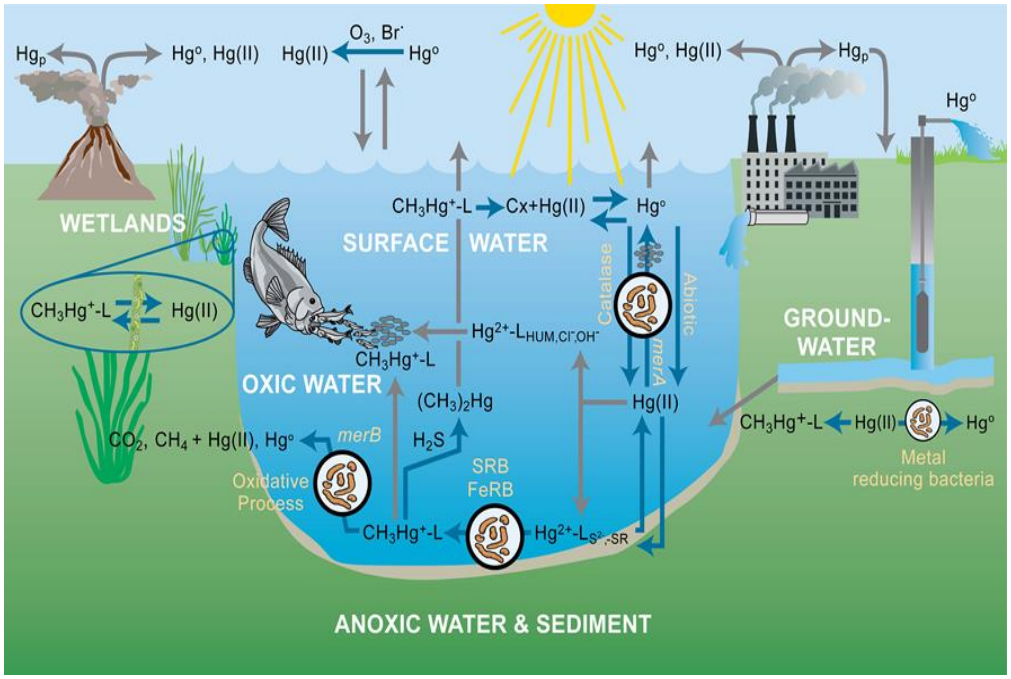

Figure 1-1: The mercury cycle. The figure shows mercury in the environment and how it is converted among its chemical forms, some with different oxidation states. Reproduced with permission of John Wiley and Sons [5].

The mercury resistance (*mer*) operon (shown in Figure 1-2) [6, 5] consists of a series of genes that together specify bacterial resistance to Hg. These genes include *merA* (mercuric reductase), *merB* (mercurial lyase), *merC*, *merD* (regulators), *merE*, *merG*, *merP* (transporter), *merR* (regulator), and *merT* (transporter).

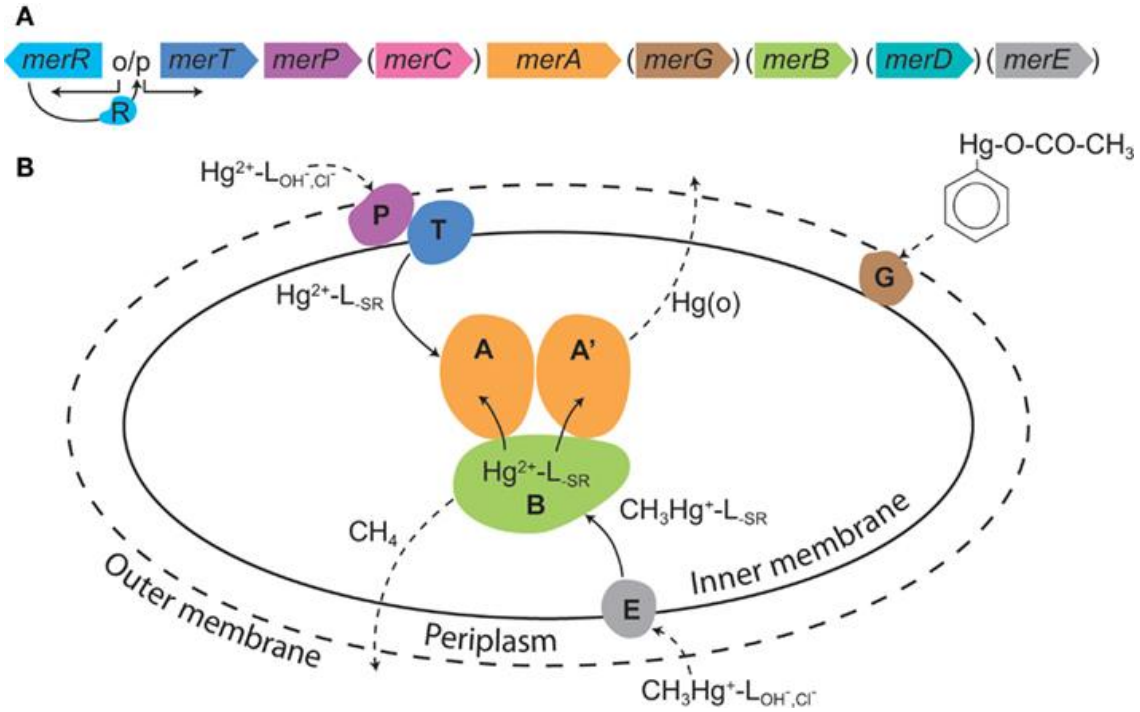

Figure 1-2: The *mer* system [6]. A and B stand for MerA and MerB respectively, P and T for MerP and MerT, G and E for MerG and MerE. L stands for ligand. Reproduced with permission of John Wiley and Sons [5].

Mercuric reductase (MerA) reduces the mercuric ion (Hg^{2+}) to volatile mercury (Hg^{0}) [7]. Mercuric reductase is a member of the flavin disulfide oxidoreductase family and was purified from both *Escherichia coli* and *Pseudomonas* sp. [7]. All MerA proteins have conserved cysteines which interact with both organic and inorganic mercurials [7], and are part of a mercury binding site, where they play a significant role in the reduction of the mercuric ion [7].

The best-characterized MerA (encoded by transposon Tn*501* [8]) is from *Pseudomonas aeruginosa* PAT [9], and its sequence consists of 560 amino acid residues [10]. Three cysteine pairs have been found essential for activity in Tn*501* as well as other MerA proteins. These cysteine pairs are located at the N-MerA (N-terminal of the MerA protein which consists of about 90 residues), at the active site, and at the carboxyl-terminus. The N-terminal cysteine pair (residues Cys11 and Cys14 according to the Tn*501* numbering), capture Hg from the environment (e.g., from other Mer proteins) and pass them to the cysteines that are located in the active site (at the catalytic core) [7]. The active site of MerA has a cysteine pair at location of Cys136 and Cys141 [11]. These cysteines have a direct role in reduction of Hg^{2+} by binding to Hg and FAD (flavin adenine dinucleotide) molecules. FAD assists with the transfer of electrons between NAD(P)H and Hg^{2+} molecules. Both NAD(P)H and Hg^{2+} are substrates of MerA, which reduces Hg^{2+} and oxidizes the NAD(P)H (equation 1). Therefore, the activity of the enzyme can be tested in two different ways, *i.e.*, mercury reduction and NAD(P)H oxidation. The third pair (residues Cys558 and Cys559) are located at the carboxy-terminus and bring the mercury to the active site for reduction [12, 13].

$$\mathbf{NAD(P)H + RS\text{-}HG\text{-}SR + H^{+} \rightarrow NAD(P^{+}) + Hg^{0} + 2RSH} \qquad \mathbf{(1)}$$

There are some observations in regard to MerA which led to the hypothesis that MerA has a thermophilic enzyme activity. These observations are: (I) phylogenies suggest that the ancestral MerA evolved in geothermal environments [4, 6], (II) Microorganisms in geothermal environments live in presence of high mercury concentrations [14], (III) Hg resistance in bacteria/archaea is very common in geothermal

environments [6, 15], and (IV) a MerA from a mesophilic bacterium, Tn*501*), shows optimal enzyme activity at 55 to 65°C [15].

The *Bacteroidetes* are a class of gram-negative bacteria, which is broadly distributed in environments rich in organic substrates such as wetlands and saltmarshes. Interestingly, they are very common in the microbial communities that live in polar regions [16]. In the bacterial MerA phylogeny, they form a lineage that is basal to all proteobacterial MerA [17]. This lineage includes *R. marinus*, a thermophile in a position basal to other *Bacteroidetes* and *Flavobacterium* sp. SOK62, a psychrophile (Figure 1-3). These two taxonomically related strains and their MerA, therefore, represent two extremes in the temperature spectrum of life.

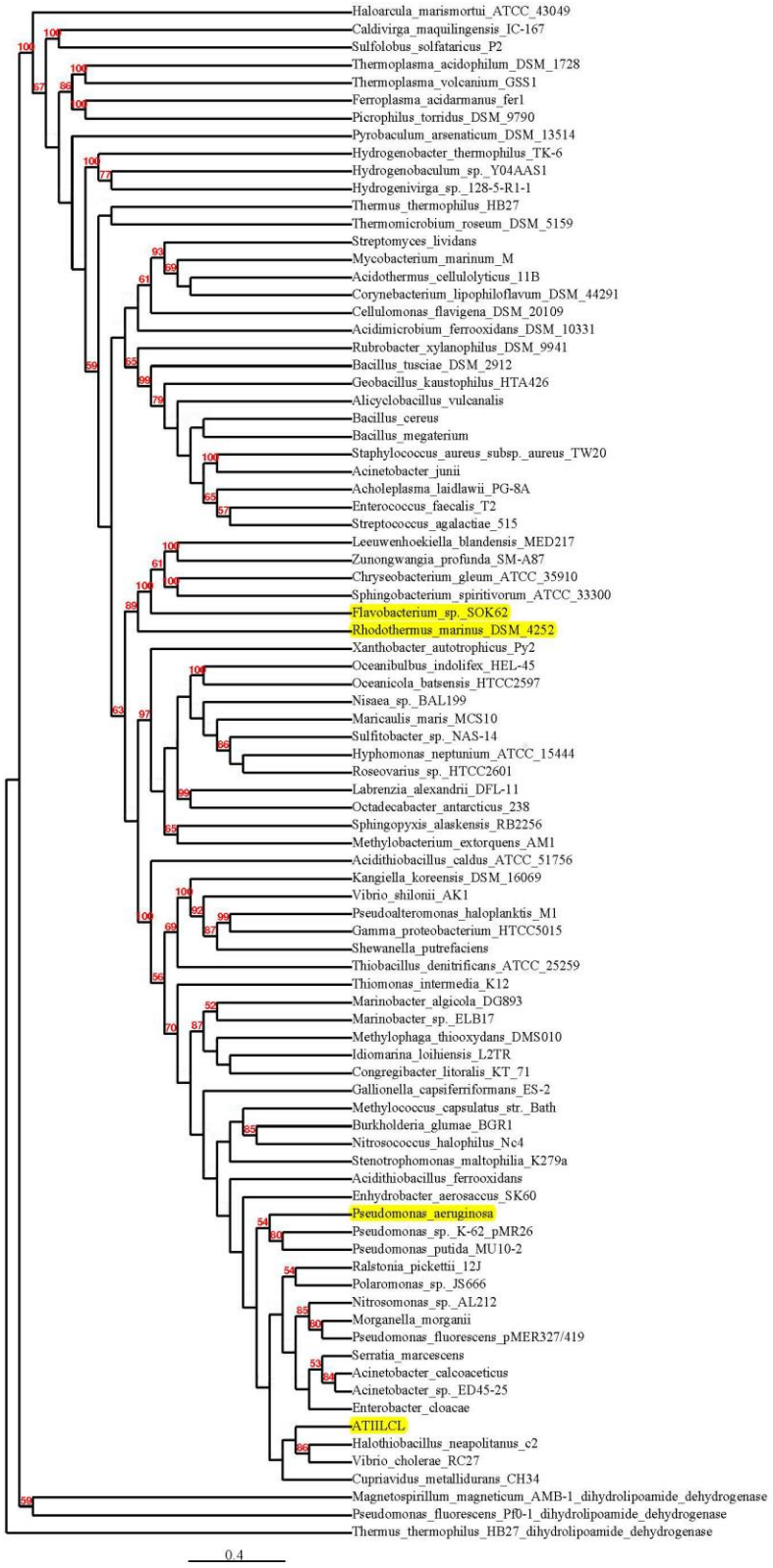

Figure 1-3: Phylogeny of MerA. The tree is made using maximum likelihood method. The red numbers indicate the boot strap which presents probability of the existence of each MerA at a certain position. Organisms that were focused on for this study are highlighted in yellow.

2 Chapter 2: Determination of optimal temperature for activity for *Rhodothermus marinus* and *Flavobacterium* sp. SOK62

2.1 Introduction

Previous work has shown that MerA is a thermophilic enzyme even in mesophilic bacteria [15]. In the MerA phylogeny (Figure 1-3), MerA in *Bacteroidetes* is a link between early lineages [1] and the more derived lineages; having MerA from closely related (phylogenetically) taxa, one a psychrophilic bacterium and the other a thermophile, is an opportunity to compare the two. This chapter discusses the methods I used to find the optimum temperature for Mer activity originating in two *Bacteroidetes,* one of them being *Flavobacterium* sp. SOK62 and the other one *Rhodothermus marinus* DSM4252. SOK62 is a psychrophile with an optimal growth temperature of 15˚C that was isolated from a snow pack in Station Nord in northeastern Greenland [17]. On the other hand, *R. marinus* is a thermophile with an optimal growth temperature of 65ºC that was isolated from a submarine alkaline freshwater hot spring in Isafjardardjup, Iceland [18].

2.2 Materials and Methods

2.2.1 Cultures and growth conditions

R. marinus DSM4252 and *Flavobacterium* sp. SOK62 [17] were used as a source for the mercuric reductase enzyme. The complete genome sequence of the thermophilic *R. marinus* DSM4252 contains an open reading frame (YP_003290665), which is

homologous to *merA*. To test if this ORF encodes for an active MerA, the gene was cloned into the expression vector pBAD202/D (Invitrogen; http://products.invitrogen.com/ivgn/product/K420201) by the students of Nancy Hamlett (Dept. of Biology, Harvey Mudd College, CA), Haley Ham and Vincent Shieh, to create plasmid pHHVS1, and by Laura Poindexter and Sung Woo Koh to create pLPSK1. In the constructed plasmids, pHHVS1 and pLPSK1, the expression of the cloned *merA* gene is controlled by the promoter of the arabinose operon. The plasmids were transformed into *E. coli* TOP10 (Invitrogen) using selection for kanamycin resistance. *E. coli* TOP10 cultures containing these plasmids were generously provided by Nancy Hamlett. Growth was initiated from frozen stocks available in the Barkay lab culture collection. *E. coli* Top 10/pHHVS1 was cultured in Luria Bertani (LB) medium at 37 ºC and *Flavobacterium* sp. SOK62 in PYG medium at 15 ºC (see Table 2-1 for media composition and growth conditions). *E. coli*/pHHVS1 was grown in presence of 100 µg/ml kanamycin to select for plasmid containing cells and *Flavobacterium* sp. SOK62 was grown in medium containing 10 µM $HgCl_2$. Table 2-1 lists the composition of the two growth media.

Table 2-1: Composition of LB and PYG media.

	Ingredients	Amount per liter
LB media	Tryptone	10 g
	yeast extract	5 g
	NaCl	5 g
	milliQ water	1000 ml
PYG media	Peptone	5gr
	Tryptone	5gr
	Yeast extract	10gr
	Glucose(dextrose)	10 gr
	Salt solution[1]	40 ml
	milliQ water	960ml

[1]Salt solution consists of 0.2 g $CaCl_2$, 0.4 g $MgSO_4.7H_2O$, 1 g K_2HPO_4, 1 gKH_2PO_4, 10 g$NaHCO_3$, 2 g NaCl, and 1000 ml milliQ water.

2.2.2 Preparation of cultures for MerA assays

To prepare the cultures, the protocols of Fox and Walsh [2] were followed with some modifications to optimize the assay for the test enzymes.

First, 1 ml of an overnight culture was transferred to a flask with 25 ml fresh medium, a 1:25 dilution (overnight culture into LB medium); $HgCl_2$ was added to SOK62 and kanamycin was added to *E. coli*/pHHVS1 to select for the tested organism. The cultures were then grown at their optimal temperature, 37 ºC for *E.* coli/pHHVS1 and at 15˚C for strain SOK62, with periodic measurements of optical density (OD) using Spectronic Genesys 20 Visible Spectrophotometer (Thermo Scientific, Waltham, MA) at 595 nm (OD_{595}) until an OD_{595} of 0.45 to 0.5 was reached. To optimize MerA production, $HgCl_2$ was added to SOK62 cultures and arabinose to *E. coli*/pHHVS1cultures for induction of their respective *merA*. For strain *E. coli*/pHHVS1, it was essential to find the optimal concentration of arabinose for induction (amplify the expression of *merA*) and several concentrations in the range 0 to 1.33 mM were tested.

Following the addition of the inducers, the cultures were incubated for additional 1 to 2 generations, about 1 hour for *E. coli*/pHHVS1 and 1 day for strain SOK62 (a slow grower). Next, the flask's contents were transferred to 250 ml centrifuge bottles (SLA-1500 Rotor) and centrifuged at 6000 rpm for 10 min (at 4 ºC) using a Sorvall RC-5B centrifuge (Thermo Scientific, Waltham, MA). The supernatant was removed, the pelleted cells were washed with a 0.85% NaCl solution, and the cell suspension was then transferred to preweighted 50 ml centrifuge bottles. Following centrifugation (SS34 rotor, for 10 minutes at 6000 rpm), the supernatant was discarded, the tube was weighted again

and the net wet weight of the pellet recorded. Lastly, cell pellets were stored at –20 ºC until the next step, the preparation of cell extracts.

2.2.3 Preparing Crude Cell Extracts

To use the pellets, they were thawed and re-suspended in re-suspension buffer. Re-suspension buffer contained 20 mM phosphate at pH 7.5 (81 parts 1 M Na_2HPO_4 and 19 parts 1 M NaH_2PO_4), 0.5 mM EDTA, 0.1 % **β**-mercaptoethanol, in filtered milliQ water. For each 0.2 gram of wet cell pellet, 1.5 ml re-suspension buffer was added [2]. The next step to extract the cell content was to break the cells. This was achieved by different methods for each of the organisms. To break the *E. coli* cells, sonication was used. In this method, cells were broken using a Misonex S-4000 sonicator (Misonex Inc. Newtown, CT) for 3 minutes at 40 watts in repeat cycles of 4 seconds sonication and 2 seconds on ice for a total of 4.5 minutes of sonication. However, the sonication method did not break the SOK62 cells, and a French press was therefore used.

The French press disrupts bacterial cells by passage of the cell suspension through a narrow orifice under pressure. The key to using the French press is that water needs to be added first to flush the cylinder for the purpose of cleaning the surface and to enhance sealing. The cell suspension was first sonicated (10 seconds) to produce a homogenous suspension and then DNAse (0.5 mg/ml) was added to loosen up clumped cell aggregates. Then, about 20 ml of the sonicated cell suspension was poured into the cylinder of an Aminco French press cell (American Instrument Company, Silver Spring, MD) and a pressure of 12000-15000 psi was applied. The resulting suspension was collected in a clean tube. Passage through the French Press was repeated 3 times to insure that cells were broken effectively [19].

Broken cell suspensions of both organisms were then centrifuged in Eppendorf tubes using a Sorvall MC-12V micro centrifuge (Thermo Scientific, Waltham, MA) at 4 ºC at 14,000 rpm for 30 minutes, and the supernatants containing the crude cell extracts were transferred to clean Eppendorf tubes. For the *E. coli* TOP10/pHHVS1extract, this step was subsequently optimized to achieve higher activities by heating the crude extract for 20 minutes at 65˚C and removing precipitated proteins by centrifugation as above.

2.2.4 MerA assay

The method used to determine the optimal temperature activity of MerA was from Fox and Walsh [2], and is described below.

Several solutions were prepared for the Fox and Walsh reductase assay buffer including 80 mM PO_4 buffer at a pH 7.5 (81 parts 1 M Na_2HPO_4 and 19 parts 1 M NaH_2PO_4), 1 mM β-mercaptoethanol, 200 µM NADPH, and 100 µM $HgCl_2$. To prepare the 200 µM NADPH or NADH stock solution, a 6.7 mg of NADPH or 5.6 mg of NADH were added, respectively, to 400 µl of milliQ H_2O. Adding 8 µl of this 20 mM solution to the 800 µl provided the final concentration of 200 µM NAD(P)H. Fox and Walsh used 100 µM $HgCl_2$ in the reductase assay, but for *E. coli* TOP10/pHHVS1 enzyme Hg concentrations above 50 µM, and for SOK62 enzyme Hg concentrations above 10 µM, were inhibitory. Therefore, reductase assays for *E. coli* TOP10/pHHVS1 and SOK62 crude cell extract preparations were carried out in a final concentration of 50 and 10 µM $HgCl_2$, respectively.

To set up each reaction, 400 µl of the 2X buffer were added to a 1 ml quartz cuvette followed by the addition of NAD(P)H, cell extract, and $HgCl_2$, filling the volume to 800 µl with MilliQ water. Various volumes of each crude extract preparation were

assayed, and each was repeated 3 times with and without Hg. To test reductase activities at various temperatures, the cuvette holder of an Aviv 14DS UV-VIS spectrophotometer (Aviv Associates, Lakewood, NJ) was connected to a Haake A81 circulating water bath (Haake instrument, Paramus NJ) to reach the desired temperatures. Reductase activities of each crude extract were measured at 0 to 100 ˚C. The spectrophotometer was set to the rate assay mode and followed the oxidation of NAD(P)H by measuring absorbance at 340 nm (the first12 seconds of the experiment). Reactions were initiated by the addition of the cell extract or the Hg substrate.

2.2.5 Optimization of the MerA assays

The Fox and Walsh reductase assay was developed with a proteobacterial MerA, while in this study I applied it to bacteroidetal MerA. Initial experiments under the published protocol indicated that assay conditions had to be optimized.

2.2.5.1 Optimizing the co-substrate, NAD(P)H

The first step of optimization was intended to select the reduced co-substrate because prior results suggested that MerA from thermophilic bacteria sometimes preferred NADH over NADPH [14, 20]. Standard MerA assays using either NADPH or NADH were therefore performed measuring activities using a Cary 300 UV/VIS spectrophotometer (Agilent Technologies, Budd Lake, NJ).

2.2.5.2 Optimizing the pH

To determine the appropriate pH for the reductase assay, the pH of the assay buffer was adjusted by varying the relative proportion of mono- and dibasic phosphate

(Table 2-2) to achieve a range of pH 6 to 8. The 2X assay buffer and the re-suspension buffer were prepared using the various phosphate stocks.

Table 2-2 Phosphate buffer concentration at different pH.

Volume (mL) of 1 M NaH_2PO_4	Volume (mL) of 1 M Na_2HPO_4	pH
815	180	6.2
510	490	6.8
280	720	7.2
130	870	7.6
53	947	8

2.2.5.3 Optimizing the thiol agents

The optimization was performed by comparing the effectiveness of different thiol agents including β-mercaptoethanol, cysteine, glutathione, and thioglycolic acid. For this purpose, thiol solutions were prepared by solubilizing the thiols in milliQ water to have an equimolar (1mM) final concentration of thiol moieties, which was the concentration that was used in the Fox and Walsh protocol [2]. β-mercaptoethanol as purchased is 14.4 M, therefore 1.4 µl were diluted to 10 mM stock solution. The details of the thiol agent preparation are shown in Table 2-3. The prepared thiol agents were added to the 2X assay and re-suspension buffers.

Table 2-3 Thiol agent stock solutions (10 mM thiol) preparation for optimizing the MerA assay.

Thiol agent	Amount of each thiol agent (mg or µl) solved in 2 ml milliQ water	Molecular weight
Glutathione (98% reduced)	6.14 mg	307.32
Thioglycolic acid	2.28 mg	114.1
β-mercaptoethanol	1.4 µl	78.13
cysteine hydrochloride (monohydrate)	3.5 mg	175.63

The next step for optimizing the thiol agent was determining the optimal concentration of the selected thiol (see Results), testing its effect on the MerA assay at the range of 0 µM-to 2mM using stock solutions of 0 to 10 mM.

2.2.6 Hg(II) reduction by growing cultures of *Flavobacterium* sp. SOK62

Because initial attempts to measure SOK62 reductase activities with cell extracts that were prepared by sonication failed, I tested whether growing cells of this strain removed Hg(II) during growth. This experiment was initiated by inoculating a petri dish containing PYG medium with frozen SOK62 stock. A single colony was then transferred to PYG broth and grown at 15°C (the optimum growth temperature for SOK62) in a low temperature incubator (Sheldon Manufacturing, Inc., Cornelius, OR) to mid log phase, when the culture was diluted 1:20 into fresh medium, dividing it into 4 flasks (100ml), three for live cultures and one flask for a heat killed control which was heated for 30 min at 80°C in a water bath. The experiment also included an uninoculated control. 10 µM $HgCl_2$ was added to all treatments. At different time intervals, a sample was removed for OD (at 595 nm) measurement to follow growth and 1 ml was placed in acid cleaned glass vials with Teflon caps for total mercury analysis. The latter were preserved by adding 0.3 ml of 25-30% BrCl solution to the vials enough to change the color of the sample to yellow/orange. Samples were checked frequently to make sure that they maintained the yellow/orange color and more BrCl was added if the samples became colorless; the amount added was then recorded. Samples were stored in the dark at 4°C until analysis [21].

2.2.7. Total Hg analysis

A Hydra AA mercury analyzer (Teledyne – Leeman Labs, Hudson, NH) was used to measure mercury remaining in the medium during culture growth. Samples were diluted 1/1000 to fit within the sensitivity, ppb range, of the instrument. Six µl aliquot of the preserved culture was pipetted, and then 150µl of 15% hydroxylamine were added as well as water to make up to 6 ml. Lastly, calculation of Hg concentration was performed for each sample (percentage of mercury remaining in growth medium). Reagents for analysis (all Trace Metal Grade and stored in vessels that had been acid-cleaned prior to use) included: 10% HCl, freshly-prepared 10% $SnCl_2$ in 10% HCl and a 2% HCl diluent. The carrier gas for analysis was Ultra High Purity Nitrogen (70-90 psi). Hg analysis was performed at a wavelength of 253.65 nm.

2.2.8. Protein assay

Protein concentrations in crude cell extracts were measured by the Bradford assay (Bio-Rad Laboratories Inc., Hercules, CA) to complete the determination of the reductase specific activities. The assays were performed in 96 well micro titer plates**.** A set of bovine serum albumin (BSA) standards in the range of 8 to 80 µg protein/ml was prepared and used to calculate protein concentrations in crude cell extracts [22]. The concentration of protein was measured, and the specific activity was calculated and expressed as mU/mg protein where U is equal to 1 µmole NAD(P)H oxidized per min.

2.2.9. Constructing a phylogenetic tree

The first step to construct the tree was to create a fasta file of MerA sequences. The sequences of strain SOK62, *R. marinus*, and the newly described thermophilic MerA

ATIICL (Sayad *et al*., 2014) were added to a previously assembled alignment file (Boyd and Barkay, 2012). Next, the fasta file was used as an input into the webpage http://www.phylogeny.fr/version2_cgi/index.cgi and the following steps were performed [23, 24]: multiple sequence alignment (using MUSCLE), curation (removing the gaps and trimming the sequences using GBLOCKS v0.91b), construction of the phylogenetic tree using a maximum likelihood method, editing the tree by using the Tree Dyn (v198.3) followed by manually adding names of organisms to each leaf in the tree (shown in Figure 1-3).

2.3 Results

2.3.1 Optimization of enzyme induction in *E. coli* TOP10/pHHVS1

Arabinose was used to induce the pBAD promoter (described in Invitrogen manual http://xray.bmc.uu.se/Courses/MPC/literature_files/pbadtopo_man.pdf) in *E. coli* TOP10/pHHVS1 in order to induce the production of the cloned *R. marinus* MerA. The promoter has a quantitative response to the concentration of arabinose, the more arabinose added the more enzyme produced. However, at high concentrations of arabinose (e.g., 1.33 mM; Figure 2-1) it has a negative effect on growth of *E. coli* TOP10/pHHVS1 relative to all other treatments, suggesting that at this level *merA* expression caused depletion of resources and led to slower growth. The result of this experiment indicated that arabinose added at the range of 1.33-133 µM had no effect on growth rate while higher concentrations inhibited growth slightly (Figure 2-1). Arabinose at 1.33 µM was therefore chosen for all subsequent experiments to produce sufficient amount of MerA for the assays.

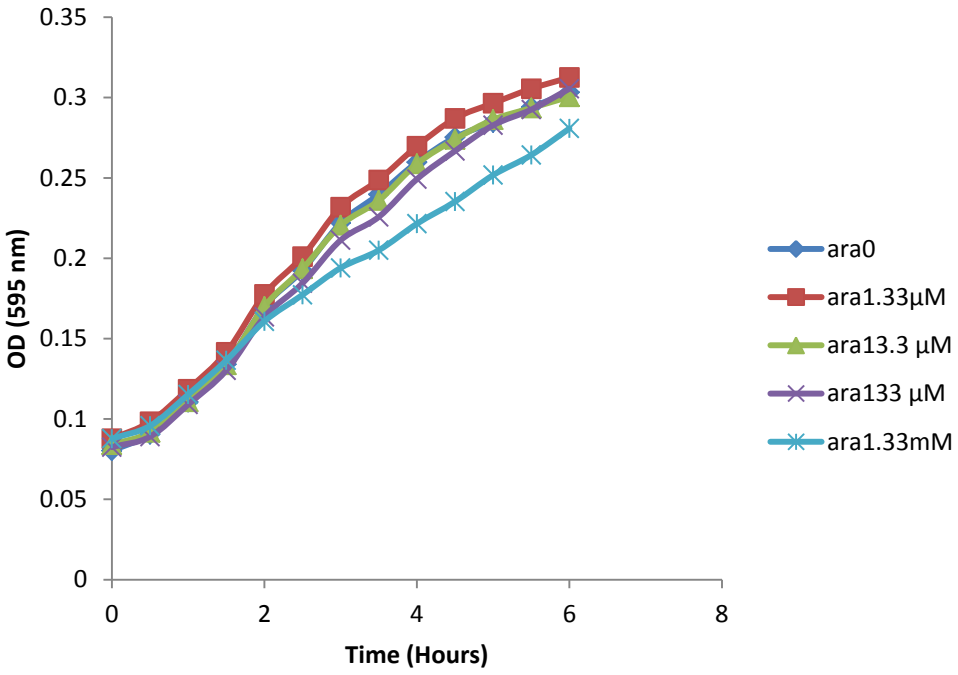

Figure 2-1 : Effect of arabinose addition on growth of *E. coli* TOP10/pHHVS1.

2.3.2 Optimization of MerA assay parameters

Figure 2-2 represents the MerA assay, which was obtained by the standardized Fox and Walsh method [2] with the crude cell extract of TPO10/pHHVS1 without optimization. The graph shows big standard deviations, which mean irreproducibility of the assay, and hence, I pursued the optimization of assay conditions for the enzymes of both *R. marinus* and *Flavobacterium* sp. SOK62.

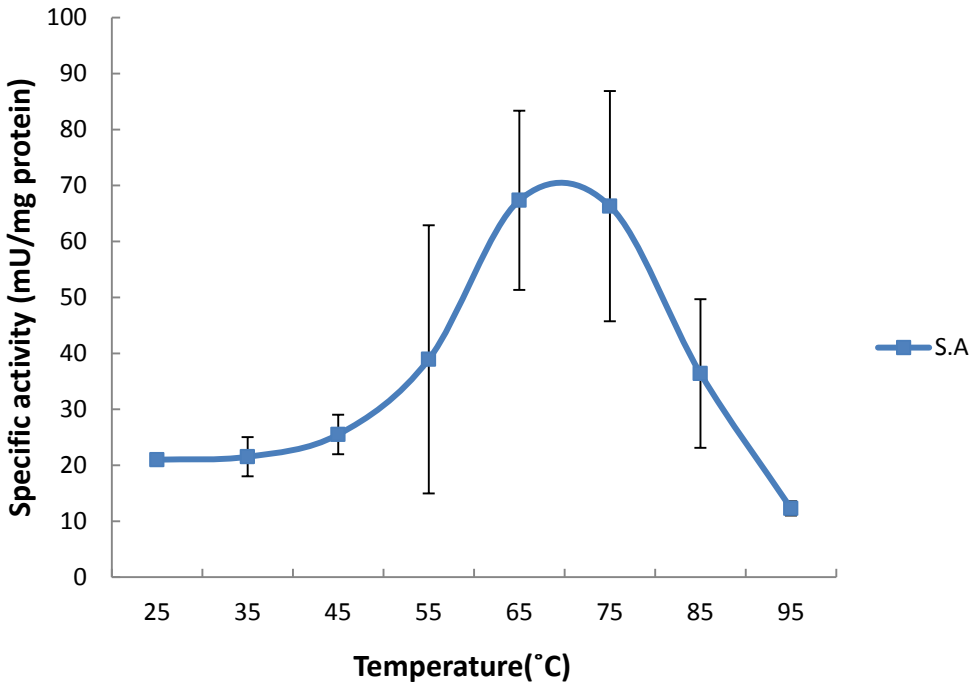

Figure 2-2: Temperature profile of *R. marinus* MerA activity before optimization of the reductase assay. The experiment was performed with 1mM β-mercaptoethanol, 80 mM PO_4 buffer at pH 7.5, 200 µM NADPH, and 50 µM $HgCl_2$

2.3.2.1 Comparing MerA activities with NADH and NADPH

First, activities with NADPH and NADH as the reduced substrates were determined. With MerA of *R. marinus*, a lower specific activity (4.1 mU/mg protein) was observed with NADPH than with NADH (52.5 mU/mg protein). On the other hand, the MerA of SOK62 had a higher specific activity when NADPH (38.5 mU/mg protein) with only 3.4 mU/mg protein when NADH was used (Figure 2-3).

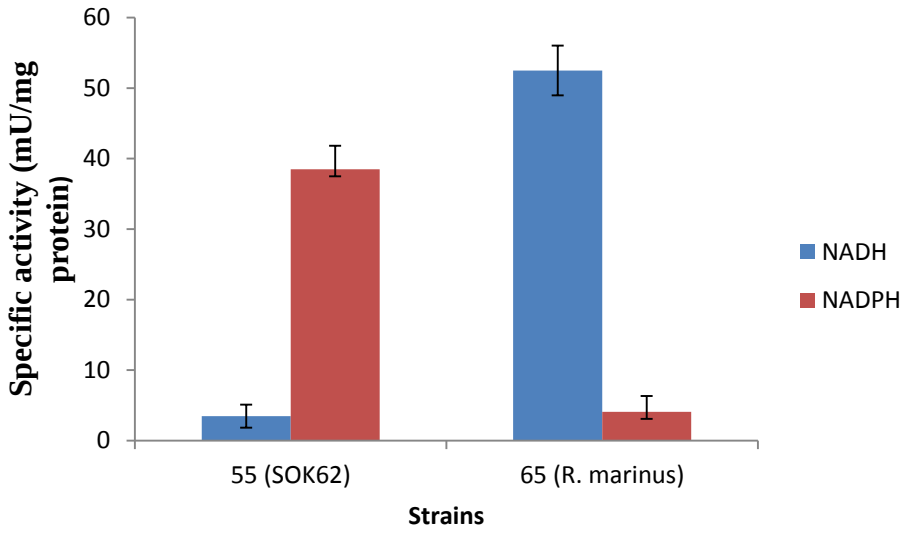

Figure 2-3: Optimization of the MerA assay by comparing activity with NADH and NADPH. The experiment was performed with 1mM β-mercaptoethanol, 80 mM PO_4 buffer at pH 7.5, 200 µM NAD(P)H, and 50 µM $HgCl_2$ for *R. marinus* and 10 µM $HgCl_2$ for SOK62.

2.3.2.2 Optimizing the activity by heating the crude extract

Previous research by Vetriani *et al.* [15] showed that *E. coli*'s crude cell extracts when heated to temperature >60 ºC formed a precipitate that interfered with the MerA assay. Therefore, I compared the specific activities of unheated and heated (at 65 ºC) extracts. The results revealed higher specific activities with the heated extract (72.6 mU/mg protein) as compared to the unheated extract (49.7 mU/mg protein). Thus, following the removal of the precipitate the cleared crude extract was 31.5% more active than the unheated extract. Protein measurements showed that 22% ($[\frac{19.2\ [mg\ protein]}{24.6\ [mg\ protein]} - 1] \times 100$) of the proteins in the original crude extract were precipitated by heat. This experiment was performed only with the TOP10/pHHVS1 extract; crude extracts of SOK62 did not show the formation of precipitate upon heating.

2.3.2.3 Optimizing the MerA assay pH

Several pH were tested to find the optimal one for activity for the *R. marinus* and *Flavobacterium* sp. SOK62 MerAs. *R. marinus* shows better activity in the pH range 6.8-7.5 (Figure 2-4), and SOK62's MerA shows better activity in the pH range 7.2-7.5. Based on these results I selected a pH 7.2 for both *R. marinus* assays and SOK62 assays.

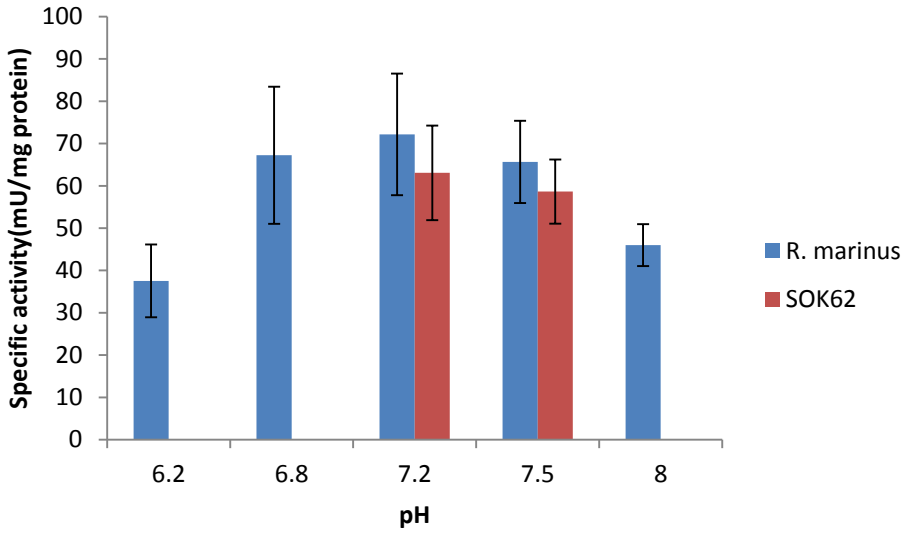

Figure 2-4: pH optimization of the MerA assays for R. marinus and SOK62. The experiment was performed with 1 mM β-mercaptoethanol, 80 mM PO4 buffer at pH 6.2-8, 200 µM NAD(P)H, and 50 µM HgCl2 for R. marinus and 10 µM HgCl2 for SOK62.

2.3.2.4 Optimizing the thiol agent and its concentration

At this stage, the activity with different thiol agents including β-mercaptoethanol, cysteine, glutathione, and thioglycolic acid was compared. Both *R. marinus* and SOK62 MerA had higher activities when cysteine was used (Figure 2-5).

The effect of cysteine concentration on MerA activity was then determined. It was observed that the highest specific activity was achieved with 5 mM cysteine (Figure 2-6)

in the case of *R. marinus*. On the other hand, for SOK62, the activity was the highest at 10 mM.

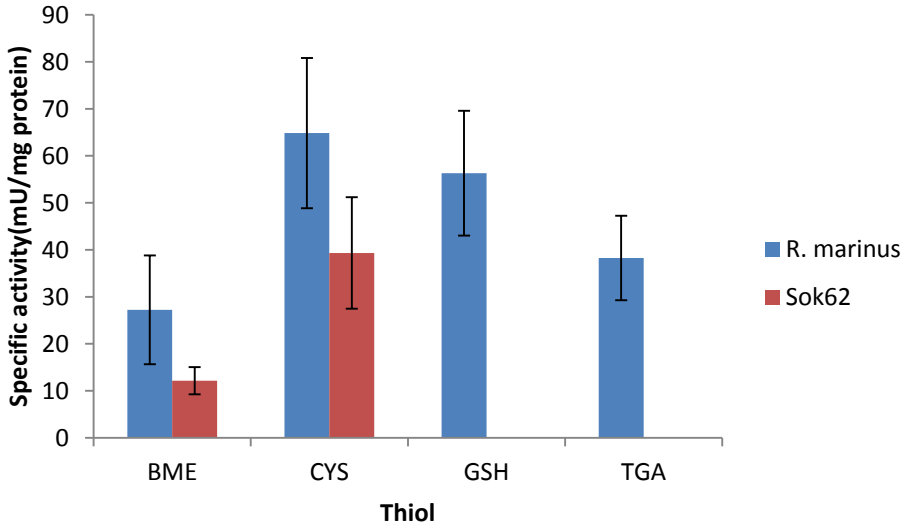

Figure 2-5 : Thiol optimization of the MerA assay for R. marinus (blue), and SOK62 (red). The experiment was performed with 1mM thiol agents such as β-mercaptoethanol (BME), cysteine (CYS), glutathione (GSH), and thioglycolic acid (TGA), 80 mM PO4 buffer at pH 7.2, 200 µM NAD(P)H, and 50 µM HgCl2 for R. marinus and 10 µM HgCl2 for SOK62.

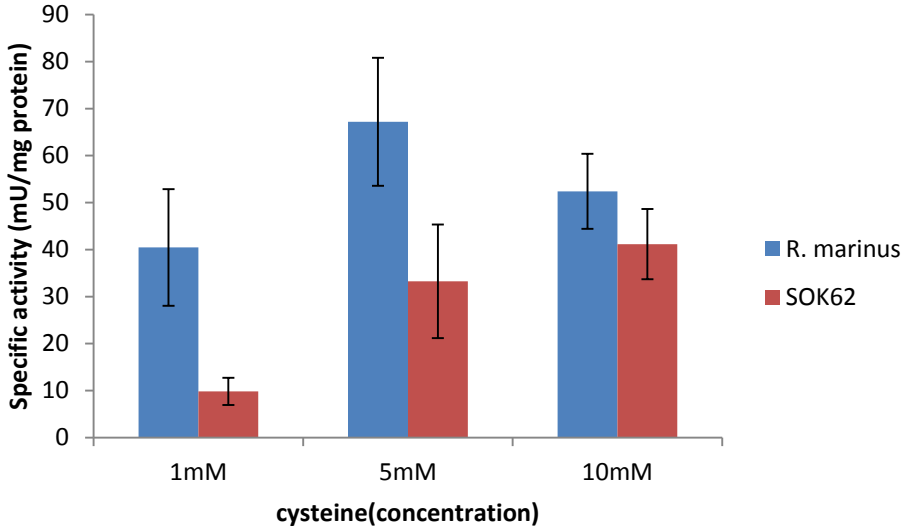

Figure 2-6 : Optimization of cysteine concentration for the MerA assay for R. marinus (blue) and SOK62 (red). The experiment was performed with cysteine in the range of 0-10 mM, 80 mM PO4 buffer at pH 7.2, 200 µM NAD(P)H, and 50 µM HgCl2 for R. marinus and 10 µM HgCl2 for SOK62.

A summary of optimizations results is shown in Table 2-4. These conditions were then employed to test the effect of temperature on MerA activities of the thermophilic and psychrophilic bacteroidatel enzymes (see below section 2.3.4).

Table 2-4: Optimized assay conditions for the reductases of strains *Flavobacterium* sp. SOK62 and *R. marinus.*

Optimized parameter	*R. marinus*	SOK62
Reduced substrate	NADH	NADPH
Heating the extract (60º C)	Yes	No
pH	7.2	7.2
Thiol agent	cysteine	cysteine
Final thiol concentration	5mM	10mM
Breaking the cell	Sonication	French press

2.3.3 *Flavobacterium* sp. SOK62 growth and mercury removal from growth media

Because *Flavobacterium* sp. SOK62 was only recently described [17] and little is known about its growth and mercury resistance, I first determined how cell growth was related to the removal of mercury from the growth medium.

The growth and mercury loss curves for SOK62 are shown in Figure 2-7. Growth was delayed until the 2nd day of incubation by which time 50% of mercury was removed. After 2 days growth continued at a consistent rate and even after 15 days, the culture did not reach stationary phase. The removal of mercury from the medium of the growing culture started immediately after inoculation, and by day 4, when growth was still at its initial stage, 75% of the added 10 µM Hg was already lost. The growth *vs.* loss analysis (Figure 2-7) was performed to test whether or not SOK62 expressed *merA*. The controls used here were heat killed cells and blank medium. Hg might have been reduced abiotically in the presence of light by photochemical reactions and also in the dark [25];

therefore, a blank (uninoculated) solution was used to determine the magnitude of abiotic loss. The other control was a heat killed culture (30 min at 80ºC) whose results showed some loss, about 20% in the first four days of the incubation. The mean and standard deviation values for Hg volatilization analysis are also shown in Figure 2-7. Thus, the *mer* system of strain SOK62 likely renders resistance to mercury by the reduction of Hg(II) to Hg(0). The effect of mercury on growth of *R. marinus* was not tested.

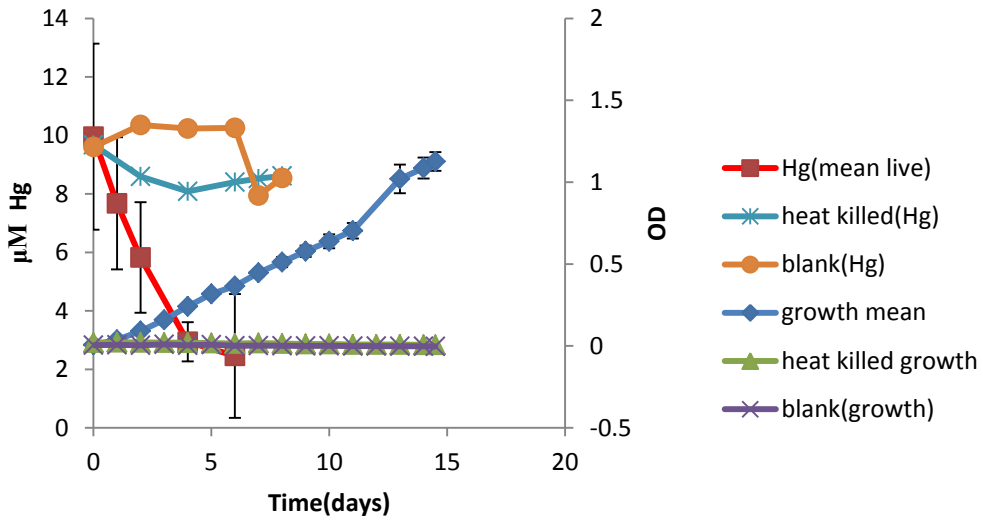

Figure 2-7: The relationship of mercury removal to growth of strain SOK62. The starting concentration for mercury volatilization was 10 µM. Means and standard deviations of 3 live replicate cultures are shown. Single incubations were set up for the killed and blank controls.

2.3.4 Effect of temperature on MerA activity using optimized assay conditions

Having optimized assay conditions (shown in Table 2-4), the assay was run at a range of temperatures for both SOK62 and *R. marinus* MerA enzymes. Because of the number of assays that were performed, I was not able to carry all of them out in one experiment. Therefore, different experiments covering different temperature ranges were

performed on different days making sure that an overlap of at least 3 temperatures was included in the experimental design of each. The final results of the effect of temperature on the specific activity for SOK62 are shown in Figure 2-8 and for *R. marinus* in Figure 2-9. The optimum temperatures for activity were 55 ºC and 65 ºC for SOK62 and *R. marinus*, respectively. The upper limits of activity for both enzymes were 95 ºC while the lower limits were 5 ºC for SOK62 and 30 ºC for *R. marinus.* For *R. marinus* the optimal temperature for MerA activity corresponded well with the bacterium's optimal growth temperature (65 ºC). For SOK62 (Møller *et al.* 2014 [17]), the activity at 55 ºC was 7 times higher than the activity at its optimal growth temperature, *i.e.*, 15 ºC (70 mU/mg protein as compared to 10 mU/mg protein). The broad temperature range for SOK62's MerA activity, 10 to 90 ºC, was also noted.

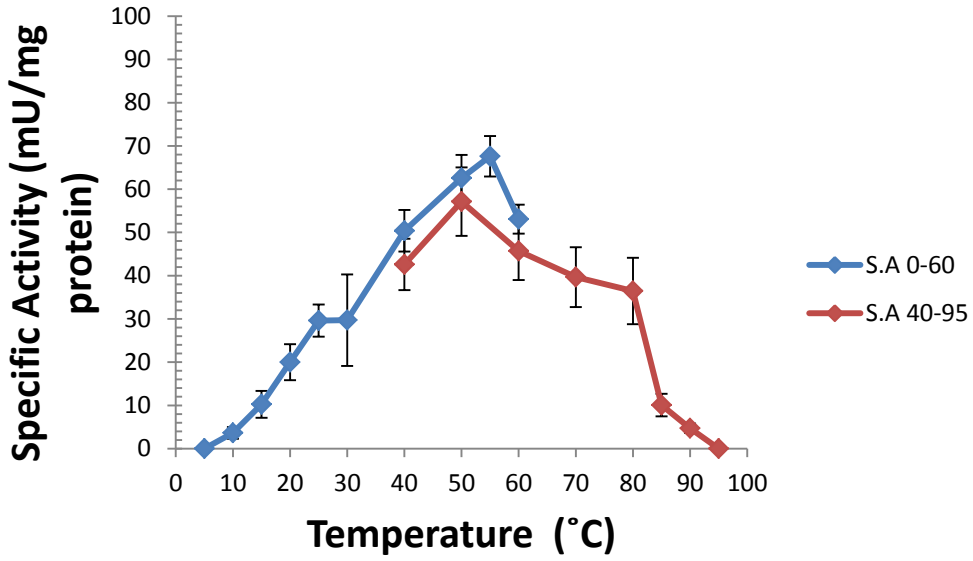

Figure 2-8: Effect of temperature on specific activity of MerA of the psychrophile *Flavobacterium* sp. SOK62. The blue curve shows activities at a temperature range of 0-60 ˚C and the red curve at 40-95 ˚C. The experiments were performed with 10 mM cysteine, 80 mM PO_4 buffer at pH 7.2, 200 µM NADPH, and 10 µM $HgCl_2$.

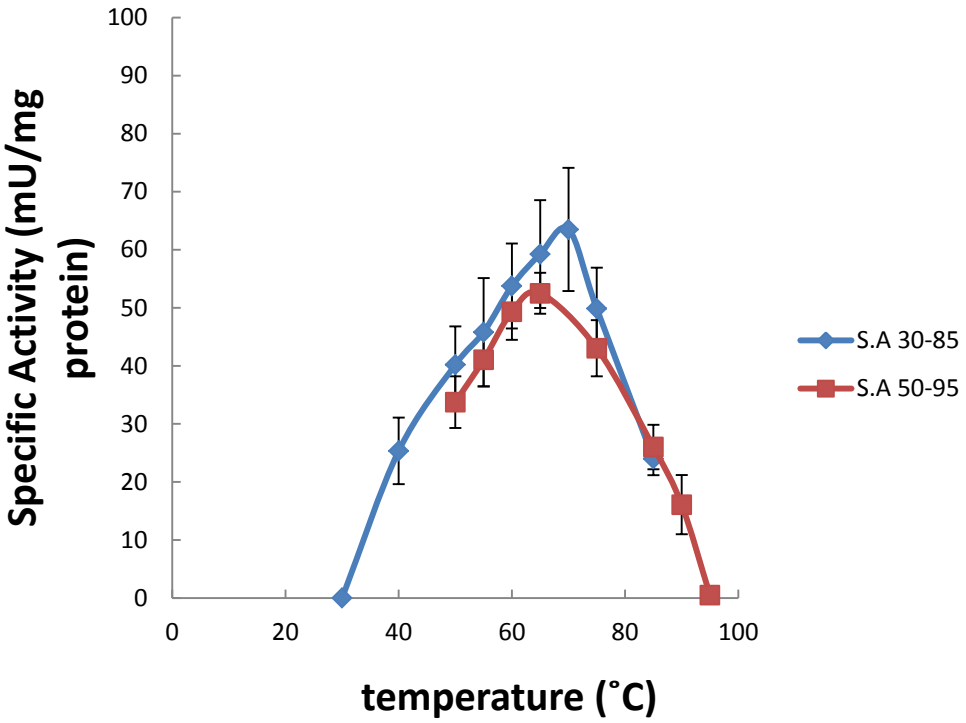

Figure 2-9: Effect of temperature on specific activity of MerA of the thermophile *R. marinus*. The red curve shows the activities at a temperature range of 50-100 °C and the blue curve activities, monitored in a second experiment, at the range of 0-85 °C. Assays were performed with 5 mM cysteine, 80 mM PO_4 buffer at pH 7.2, 200 µM NADH, and 50 µM $HgCl_2$.

2.4 Discussion/Conclusion

An optimum activity graph for the three classes of MerA that were described in recent years, originating in a psychrophile, a mesophile ([15], [26]), and thermophiles ([26], [14]) is shown in Figure 2-10.

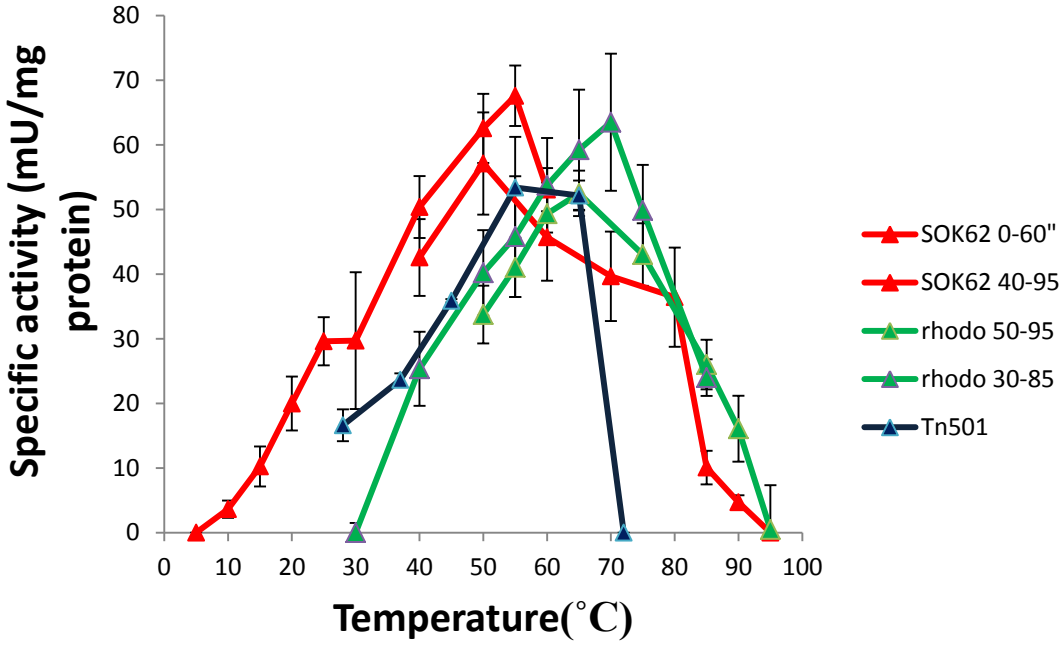

Figure 2-10: Comparison of the activity of MerA of SOK62, *R. marinus*, and Tn*501*. The red curves show the activity of SOK62, the green curves for *R. marinus*, and black curve for Tn*501*. The Tn*501* result was multiplied by 1.5 to facilitate the comparison [26].

It is clear that the temperature range of activities for the enzymes of the extremophile (either thermophile or psychrophyle) is broader than that of the mesophile (Tn*501*), 72 ºC to 37 ºC (Figure 2-10, and Figure 2-11).

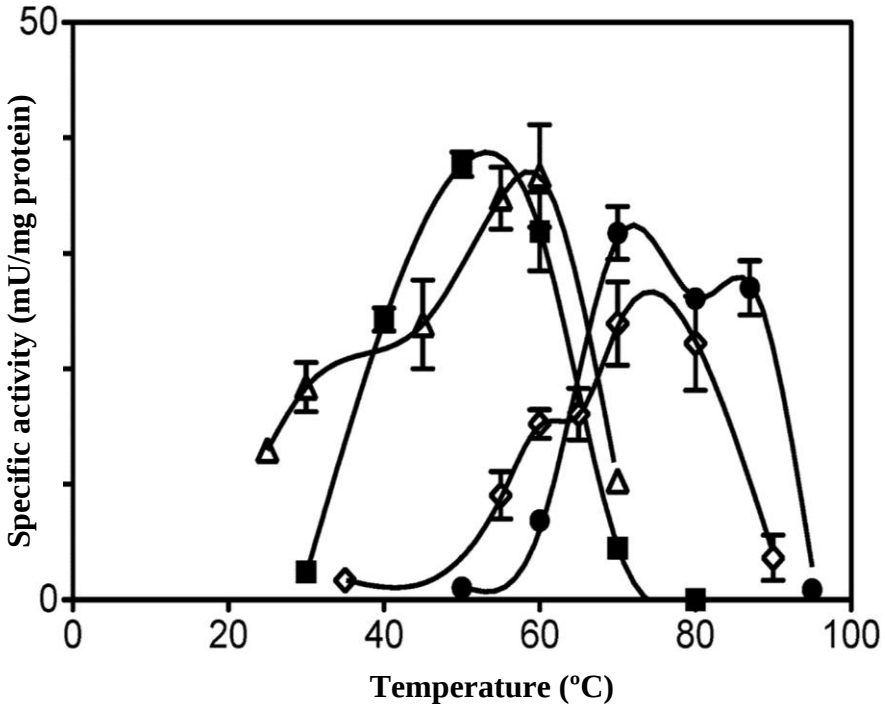

Figure 2-11: The specific activities of *Hydrogenobaculum* sp. Y04AAS1 (■), *Hydrogenivirga sp.* 128-5-R1-1 (●),Tn*501*(Δ), and *Thermus thermophilus* (◊). This figure is reprinted from Freedman *et al*. Reproduced with permission of American Society for Microbiology [14].

The phylogeny of MerA shows that the MerA originated in thermophiles (Figure 1-3). Then it evolved into an enzyme that could act at mesophilic temperatures (as in *P. aeruginosa* Tn*501*); this evolution seems to have resulted in a substantial narrowing of the temperature range of MerA (Figure 2-10 and Figure 2-11). The evolutionary distance between the MerA of the two extremophilic *Bacteroidetes*, *i.e.,* SOK62 and *R. marinus,* is shorter compared with their distance from the mesophile (Tn*501*) (Figure 1-3). It is possible that adaptation to activity at lower temperature in SOK62 was associated with an expansion of the temperature range of activity of an otherwise thermophilic enzyme along with a longer evolution time than for the transition from a thermophilic to mesophilic environment that is represented by MerA of Tn*501*.

Figure 2-10 supports the hypothesis of a thermophilic origin for MerA. All three enzymes have optimum temperatures for activity in a thermophilic range even though the optimum growth temperatures of the organisms that are not thermophiles is lower, as is evidenced from the data for *P. aeruginosa* hosting Tn*501* and *Flavobacterium* sp. SOK62.

Mercury from atmospheric deposition in polar regions is highly bioavailable [27] and microbes containing MerA (for example, strain SOK62) may play an important role in mercury detoxification in these environments.

Among all of the thermophiles such as *Hydrogenobaculum* sp. strain Y04AAS1 (optimal activity at 50°C) [14], *Hydrogenivirga* sp. strain 128-5-R1-1(at 70°C) [14], *Thermus thermophilus* (at 70ºC) [26], and *R. marinus* (at 65ºC), the optimal MerA activities were identical or close to the bacteria's optimal growth temperatures.

Interestingly, a recent thermophilic MerA was isolated from a metagenomic clone library that was obtained from a brine pool at the Atlantis II depth in the Red Sea [28]. When added to the MerA phylogeny, this sequence (ATII-LCL) represents a very recent derivation of MerA (Figure 1-3). This enzyme is highly temperature stable but its optimal temperature for MerA activity has not been determined. This enzyme's optimal temperature for activity and the temperatures range at which activity can occur might shed a broader light on the evolution of a thermophilic MerA into a mesophilic one and back to a thermophilic enzyme.

3 Chapter 3: Homology modeling of thermophilic and psychrophilic MerA

3.1 Introduction

Microorganisms could be categorized based on their optimal growth conditions such as psychrophiles (microorganisms with optimal growth temperature below 20 °C and no growth above 20 ºC), mesophiles (microorganisms with optimal growth temperature between 20-45°C), thermophiles (microorganisms with optimal growth temperature between 45-80°C), and hyper thermophiles (microorganisms which can grow above 80 °C) [29]. Thermophilic bacterial proteins usually show high intrinsic thermal stability [30], but the structures are analogous to mesophilic homologues. Based on the protein structures, one of the rules that are generally observed is that the number of ion pairs will increase with higher temperatures [31, 30]. In contrast, proteins from cold adapted or psychrophilic organisms have greater flexibility [32]. The proteins from psychrophilic bacteria have more short or neutral side chains compared to thermophiles or mesophiles [29]. The crystal structure of Tn501 MerA was used as a mesophilic template Ledwidge et al [33] to create the structure of the psychrophile and thermophile homologs. The bacteria hosting MerA from Tn501, strain SOK62, and *R. marinus* are mesophile, psychrophile, and thermophile, respectively. The sequences of the three proteins are shown in Figure 3-1, Figure 3-2, and Figure 3-3. Comparative modeling was undertaken in an effort to correlate functional differences among the proteins with structural features.

We examined the positions of polar, aromatic, charged, and nonpolar residues. In addition, their distances to the active site and other mercury binding domains were determined (at the N-MerA motif or the C-terminus). Furthermore, the location of each residue in the secondary structures i.e., in α-helices, β-sheets, or in the loops was analyzed. Finally, the residues' locations on the surface or isolated in the core of protein were determined.

3.2 Material and methods

The steps to create a three dimensional protein model based on amino acid sequence homology are explained in the following sections.

3.2.1 Loading in a sequence file

The amino acid sequences of *R. marinus* and SOK62 are shown in Figure 3-1 and Figure 3-2, respectively.

```
  1 mkkilelrig gmtcthcart ieqalmrvpg vvraqvpgwq sgravvtweg davdaealrk
 61 avaqaghgyr leawevvrei gsetptrsgs dridydllii gggsaafaaa lrarelgfrs
121 livndglppg gtcvnvgcvp skaliraaea hhraahhpfa girstsrved fgavigqvqa
181 ltdelrrhky ldlidgrqiv fregrarlag ptaiqvgdet itgravliat gsrtalppvp
241 gladgpyltn etlyrlsvlp ehlivlgggy iglenaqafa rlgsrvtvle llpqilpqed
301 advaealtty lqaegidiqt earvvevawq egsvvvtyer dgathrlegs hllvatgrrg
361 ntddlgleal giatdrqgfl qvdetlrtav ptvlgagdvi gnppfvytaa yegqlaaena
421 lmnrhevrdy salpwvvftd pqvagvglse reaqaagley etsvlplsev pralvgrdtr
481 gfikllrdpv tdrllgariv apeggelvme lslalryeip vselarrfhp yltwseavkl
541 aalgftkdvr qlsccav
```

Figure 3-1: The amino acid sequence of MerA of *R. marinus*. http://www.ncbi.nlm.nih.gov/protein/ACY48277.1

```
  1 mktenikldi agmtcdhcat giekmltkne gvtevkvsyq ngscecsfdp sktskeeiin
 61 tinstknykv ahtaetkccn tnanhfdlii igggsaafsa aikaeslgls tlmvnggldf
121 ggtcvnvgcv psktliraae tayhathsnf sgikpkgvai dfaqvikdkk qlvatlqkkk
181 ymdvvsdfhn lkmltgwaef ldtktivvdg kvkytalkfi iatgattnip iieglnevgf
241 ltnvslfdle ekpesmtimg agyigleiam aynrlgvkvr iieftdrvlr tqtpdiseal
301 etqmrnegie ilpnfravkf dkkgnetiih ckcpdgsftq iiekgkvvva sgttpnmqkl
361 glqniglela ktghilvnek metnlpniya vgdvtntpaf vytaafegki avenaftgan
421 neadysslpw vvftdpqvag agldeaqaev qnipfevskl elnnvpraia andtrgfikl
481 irntetdkli garivapegg eliqqlsmai kynitvkela esfypyltlg egiklaaitf
541 gkdvaklscc as
```

Figure 3-2: The amino acid sequence of MerA of *Flavobacterium* sp SOK62. http://www.ncbi.nlm.nih.gov/protein/485658516

The PDB files 1zk7 (for core protein) and 2kt2 (for N-merA) were used from the clustalw multiple alignments. Similar or identical residues were found in many places. Modeling for MerA of SOK62 and *Rhodothermus marinus* is shown in Table 3-1.

Table 3-1 : Query information of the models

sequence	SOK62	*R. marinus4252*
Query ID	1c1/19109	1c1/48200
Query length	552	557

For using the sequences as a query into InsightII, they had to be converted to PIR format (FASTA format could not be used).

3.2.2 Searching for a template

The amino acid sequences of SOK62 and R. marinus were used as an input to a BLAST search against the Protein Data bank. The mercuric reductase of Tn501 ([Pseudomonas sp. K-62]) had the largest percentage of similarity (1ZK7 40%), and

therefore served as the template for homology modeling. The amino acid sequence of Pseudomonas sp. K-62 MerA is shown in Figure 3-2.

```
  1 mthlkitgmt cdscaahvke alekvpgvqs alvsypkgta qlaivpgtsp daltaavagl
 61 gykatladap ladnrvglld kvrgwmaaae khsgneppvq vavigsggaa maaalkaveq
121 gaqvtlierg tiggtcvnvg cvpskimira ahiahlrres pfdggiaatv ptidrsklla
181 qqqarvdelr hakyegilgg npaitvvhge arfkddqslt vrlneggerv vmfdrclvat
241 gaspavppip glkespywts tealasdtip erlavigssv valelaqafa rlgskvtvla
301 rntlffredp aigeavtaaf raegievleh tqasqvahmd gefvlttthg elradkllva
361 tgrtpntrsl aldaagvtvn aqgaividqg mrtsnpniya agdctdqpqf vyvaaaagtr
421 aainmtggda aldltampav vftdpqvatv gyseaeahhd gietdsrtlt ldnvpralan
481 fdtrgfiklv ieegshrlig vqavapeage liqtaalair nrmtvqelad qlfpyltmve
541 glklaaqtfn kdvkqlscca g
```

Figure 3-3: The amino acid sequence of MerA from Tn*501*. http://www.ncbi.nlm.nih.gov/protein/P00392.1

3.2.3 Loading in the PDB file for template

At this step, the program InsightII (Accelrys) was used. The known structure of Tn*501* (PDB file 1ZK7) was read in followed by the sequences of SOK62 or *R. marinus*, which served as the queries and which were converter to PIR format for input.

3.2.4 Aligning the sequences

For each query the InsightII facilities were used to form the sequence alignments. Aligned sequences of template and query were enclosed in Insight II "boxes." were created. Boxes were frozen before the following step, *i.e.*, assigning the coordinates.

3.2.5 Assigning coordinates to the structurally conserved regions

Identical residues were assigned identical coordinates. Non-identical aligned residues were assigned identical backbone coordinates. The coordinates of their side

chains were taken from the program's rotamer library. This step was repeated for each box.

3.2.6 Creating loops

Residues which had not been aligned and initial coordinates assigned as above were next constructed. The PDB database was searched for known structures having loops connecting secondary structures whose lengths equaled those of the query. The loops also were chosen so that their end-to end distances matched the attachment points to the model and so that their attachmemnts did not produce abrupt changes in the polypeptide direction that violated standard geometry. Reasonable conformers were found, and initial loop coordinates were assigned.

3.2.7 Refining the structures by energy minimization

The steps up to this poing usually create some steric clashes and other violations of the normal properties of well folded proteins. These are relieved by energy minimization. In order to minimize a structure, the potential of each atom must be specified. In order to specify the potentials, all of the hydrogens must be explicitlypresent. Therefore, hydrogens were added to the models. After adding the hydrogens, models were minimized to convergence in the presence of a shell of water molecules to simulate the protein's normal aqueous environment. The default settings in Insight II were used for the minimization. The resulting models were saved as PDB files.

The bond lengths and bond angles were checked to be sure the geometry conformed to normal molecular structure. Minimization of the molecule was started with

100 iterations. Then, the models were "soaked" into water. In the last run, 100,000 iterations were initiated. The energy converged to a minimum as shown in Table 3-2.

Table 3-2: Iteration of the models.

Minimization	SOK62	*R. marinus*
Iterations to convergence	12460	31142

3.2.8 Solvent accessible surface areas and molecular volumes

Solvent accessible surface areas were calculated by the method of Lee and Richards using the program ACCESS [34]. Since ACCESS uses heavy atoms only hydrogens were stripped from the PDB files. ACCESS yields one line of output for each heavy atom in the molecule, so to analyze the results in terms of atom type, the output files were input to a program called BINS, which classifies each atom as to whether is it aromatic, aliphatic, polar charged or polar uncharged. BINS then tabulate the results. It is described in Kajander *et al*. [35].

Richards's program VOLUME was used to compute molecular volumes, the output being tabulated and formatted for analysis by Richards's program VOLFMT [34], [36].

3.3 Results

Comparison of amino acid residues of the 3 sequences (shown in Table 3-4, and Table 3-5), reveals that SOK62 has more bulky (aromatic R group) and polar residues than MerA of the mesophile or thermophile.

3.3.1 Analyzing the models

The models are shown in Figure 3-4, Figure 3-5,Figure 3-6, and Figure 3-7, the images having been constructed with Pymol. They were analyzed as follows:

The residues in each secondary structure (the alpha helices and beta sheets) was determined by counting the residues that were exist in each secondary structures, the numbers being shown in Table 3-5. Each type of residue in each model was counted based on polarity and charge (shown in Table 3-4). The number of each kind of residue was counted (shown in Figure 3-8). The gly-x-gly area of each residue was calculated (shown in Table 3-6, Table 3-7, and Table 3-8).

ACCESS and BINS were used not only to determine the solvent accessible surface areas but also to estimate the degree of burial of each protein atom. To estimate percentage burial, a reference structure representing full exposure was created from 20 tripeptides of the form gly-X-gly, where X represented each of the amino acids in turn. The backbone conformations of these were set to the phi-pso angles of a fully extended strand except for proline, for which the angles of polyproline II were used (Table 3-9).

The volumes were calculated and the output organized by amino acid as described above. For 1ZKNH1, there were 132 atoms of the total number of atoms in the protein, whose volumes could not be calculated by the Richards algorithm for geometric reasons. These were flagged and deleted. Fortunately they would constitute only a small fraction of the protein’s volume. The results for are shown in Table 3-3

Table 3-3: Protein volumes ($Å^3$)

	1ZKNH2 (Tn*501*)	Flavo1.vaa (SOK62)	Rhodonh1.vaa (*R. marinus*)
Main chain	30996	28771	28757
Side chains	35131	39193	38280
All	66128	67963	67038

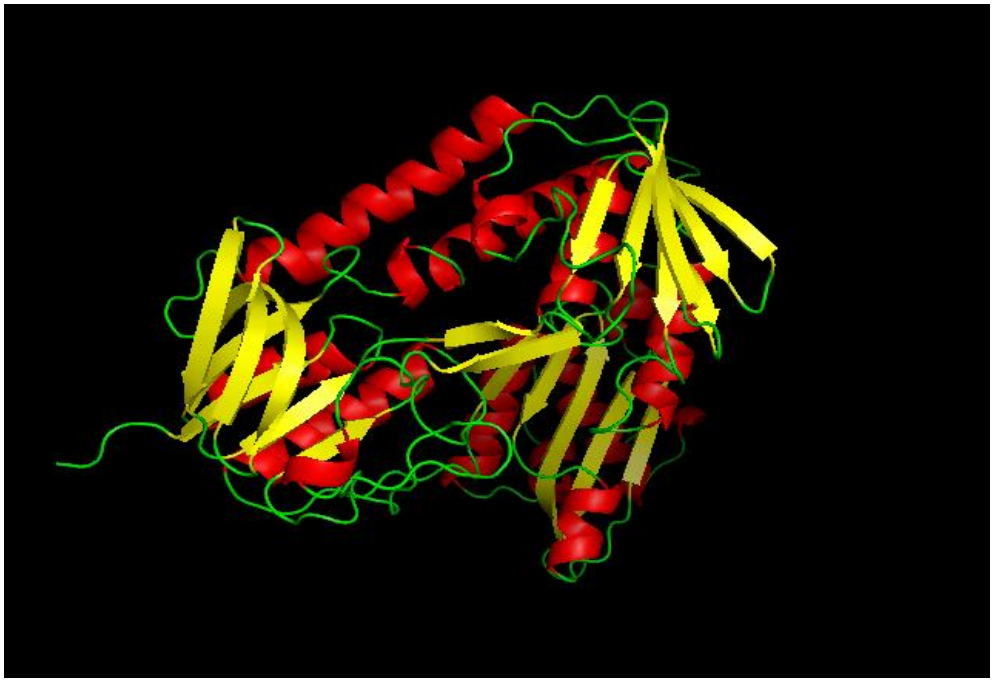

Figure 3-4: The core MerA protein. The structure of MerA of Tn501 was done by Ledwidge *et al* [33] .Its PDB file is named 1ZK7.

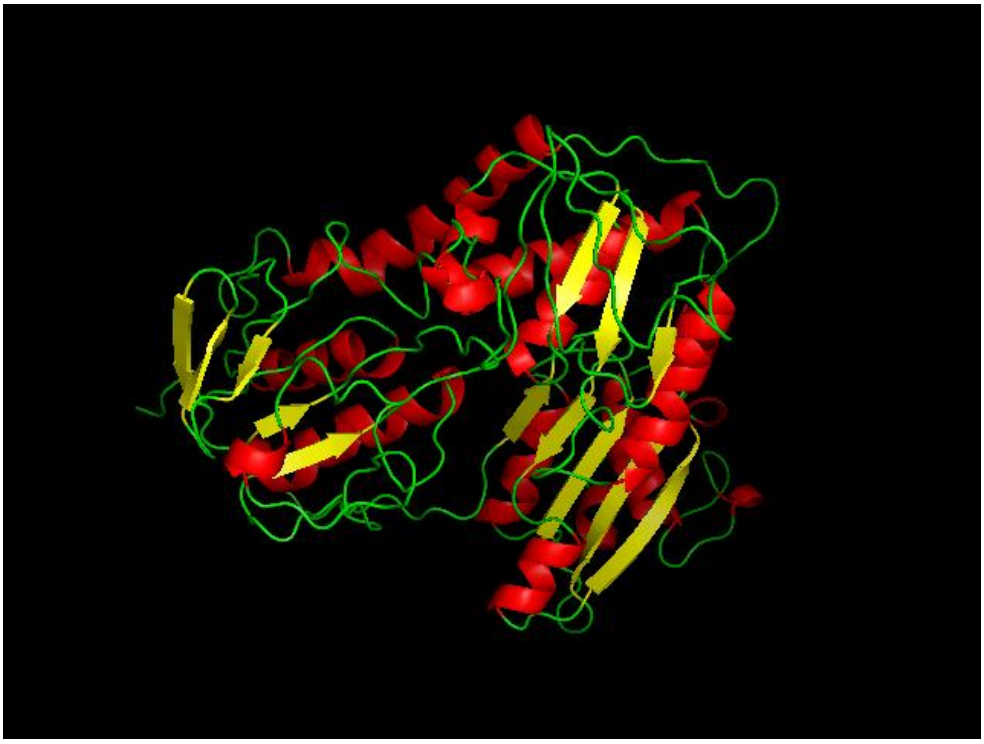

Figure 3-5: MerA model of SOK62.

Figure 3-6: MerA model of *R. marinus.*

Table 3-4: Comparison of amino acid residues among psychrophile (SOK62), thermophile (*R. marinus*), and mesophile (Tn*501*) MerA.

#	Amino Acids	# & (%) of Tn*501*	# & (%) of SOK62	# & (%) of *R. marinus*
1	Nonpolar, aliphatic R groups (G,A,V,L,I,M)	228(48.8%)	213(45.2%)	228(48.8%)
2	Polar, uncharged R groups (S,T,C,N,Q)	117(25.1%)	119(25.3%)	98(30.0%)
3	Aromatic R groups (F,Y,W)	21(4.5%)	35(7.4%)	28(6.0%)
4	Positively charged R groups (K,R,H)	49(10.5%)	52(11.0%)	54(11.6%)
5	Negatively charged R groups (D,E)	52(11.1%)	52(11.0%)	59(12.6%)
6	TOTAL	467 (100%)	471(100%)	467(100%)

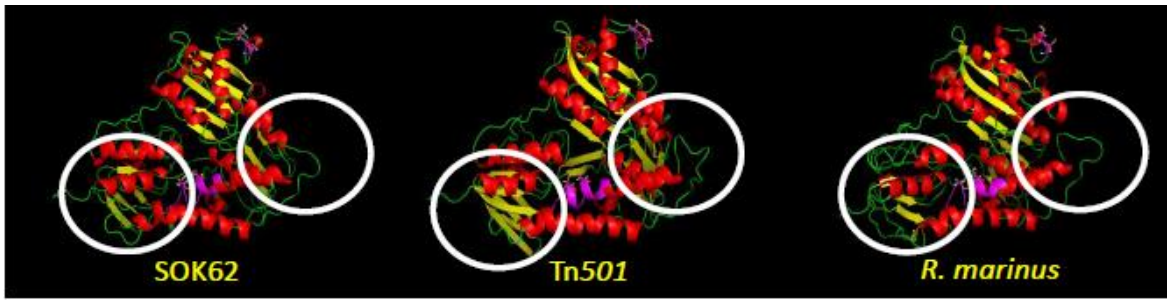

Figure 3-7: Models of MerA of SOK62 and *R. marinus* created based on homology to Tn*501*'s MerA template. α helices are in red, β sheets in yellow, loops in green, and the active site highlighted in purp0%)le helices. White circles are regions where the structures of the three MerA vary.

Table 3-5: Comparison of structural properties of psychrophile (SOK62), thermophile (*R. marinus*), and mesophile (Tn*501*) MerA based on the number of residues assigned to each secondary structure.

	# & (%) of α residues	# & (%) of β residues	# & (%) of loop residues	total
SOK62 (P)	158 (33.5%)	61 (13.0%)	252 (53.5%)	471 (100%)
Tn*501* (M)	158 (33.8%)	124 (26.6%)	185 (39.6%)	467 (100%)
R. marinus (T)	149 (31.9%)	76 (16.3%)	242 (51.8%)	467 (100%)

Table 3-6: Solvent accessible surface areas of the extended polypeptide reference conformation for MerA of Tn*501*.

"X"	AL	AR	PU	PC	PHOB	PHIL	Total	"X"	N	AL	AR	PU	PC	PHOB	PHIL	Total
	area	area	area	area	area	area	area			area	area	area	area	area	area	area
ALA	79.3	0.0	34.9	0.0	79.3	34.9	114.2	ALA	70	5551.0	0.0	2443.0	0.0	5551.0	2443.0	7994.0
ARG	84.0	0.0	34.1	141.5	84.0	175.6	259.6	ARG	27	2268.0	0.0	920.7	3820.5	2268.0	4741.2	7009.2
ASN	38.0	0.0	116.4	0.0	38.0	116.4	154.4	ASN	13	494.0	0.0	1513.2	0.0	494.0	1513.2	2007.2
ASP	38.1	0.0	34.5	79.8	38.1	114.3	152.4	ASP	23	876.3	0.0	793.5	1835.4	876.3	2628.9	3505.2
CYS	106.3	0.0	34.3	0.0	106.3	34.3	140.6	CYS	6	637.8	0.0	205.8	0.0	637.8	205.8	843.6
GLN	55.6	0.0	139.6	0.0	55.6	139.6	195.2	GLN	21	1167.6	0.0	2931.6	0.0	1167.6	2931.6	4099.2
GLU	57.6	0.0	34.1	94.6	57.6	128.7	186.3	GLU	29	1670.4	0.0	988.9	2743.4	1670.4	3732.3	5402.7
GLY	40.6	0.0	45.3	0.0	40.6	45.3	85.9	GLY	40	1624.0	0.0	1812.0	0.0	1624.0	1812.0	3436.0
HIS	33.0	82.4	49.7	32.5	115.4	82.2	197.6	HIS	10	330.0	824.0	497.0	325.0	1154.0	822.0	1976.0
ILE	156.1	0.0	28.3	0.0	156.1	28.3	184.4	ILE	25	3902.5	0.0	707.5	0.0	3902.5	707.5	4610.0
LEU	152.5	0.0	34.0	0.0	152.5	34.0	186.5	LEU	40	6100.0	0.0	1360.0	0.0	6100.0	1360.0	7460.0
LYS	114.5	0.0	33.8	78.2	114.5	112.0	226.5	LYS	12	1374.0	0.0	405.6	938.4	1374.0	1344.0	2718.0
MET	167.1	0.0	34.0	0.0	167.1	34.0	201.1	MET	10	1671.0	0.0	340.0	0.0	1671.0	340.0	2011.0
PHE	28.3	157.4	34.0	0.0	185.7	34.0	219.7	PHE	14	396.2	2203.6	476.0	0.0	2599.8	476.0	3075.8
PRO	122.8	0.0	22.5	0.0	122.8	22.5	145.2	PRO	21	2577.8	0.0	471.5	0.0	2577.8	471.5	3049.2
SER	45.0	0.0	83.6	0.0	45.0	83.6	128.6	SER	19	855.0	0.0	1588.4	0.0	855.0	1588.4	2443.4
THR	77.3	0.0	71.7	0.0	77.3	71.7	149.0	THR	37	2860.1	0.0	2652.9	0.0	2860.1	2652.9	5513.0
TRP	29.3	160.8	65.8	0.0	190.1	65.8	255.9	TRP	1	29.3	160.8	65.8	0.0	190.1	65.8	255.9
TYR	28.1	121.5	87.2	0.0	149.6	87.2	236.8	TYR	6	168.6	729.0	523.2	0.0	897.6	523.2	1420.8
VAL	134.7	0.0	29.9	0.0	134.7	29.9	164.6	VAL	43	5792.1	0.0	1285.7	0.0	5792.1	1285.7	7077.8
								Totals:	467	40346	3917	21982	9663	44263	31645	75908
1zk7																

The left side of the table gives the solvent accessible surface area of the central residue in the tripeptide gly-X-gly in the extended form. AL = aliphatic, AR = aromatic, PU = polar uncharged, while PC = polar charged. Each of these refers to the atom type within the residue, not to the entire residue .The column labeled N gives the number of residues of the given type in the protein. Thus for alanine, for which N = 70, the aliphatic area for ala in the tripeptide, 79.3 $Å^2$, multiplied by 70 gives the total aliphatic surface area, 5551.0 $Å^2$, over all the alanines in the protein if it were to be in a fully extended conformation. This is used as a reference for computation of percentage burial.

Table 3-7: Solvent accessible surface areas of the extended polypeptide reference conformation for MerA of SOK62.

"X"	AL	AR	PU	PC	PHOB	PHIL	Total	"X"	N	AL	AR	PU	PC	PHOB	PHIL	Total
	area	area	area	area	area	area	area			area	area	area	area	area	area	area
ALA	79.3	0.0	34.9	0.0	79.3	34.9	114.2	ALA	47	3727.1	0.0	1640.3	0.0	3727.1	1640.3	5367.4
ARG	84.0	0.0	34.1	141.5	84.0	175.6	259.6	ARG	11	924.0	0.0	375.1	1556.5	924.0	1931.6	2855.6
ASN	38.0	0.0	116.4	0.0	38.0	116.4	154.4	ASN	28	1064.0	0.0	3259.2	0.0	1064.0	3259.2	4323.2
ASP	38.1	0.0	34.5	79.8	38.1	114.3	152.4	ASP	20	762.0	0.0	690.0	1596.0	762.0	2286.0	3048.0
CYS	106.3	0.0	34.3	0.0	106.3	34.3	140.6	CYS	6	637.8	0.0	205.8	0.0	637.8	205.8	843.6
GLN	55.6	0.0	139.6	0.0	55.6	139.6	195.2	GLN	13	722.8	0.0	1814.8	0.0	722.8	1814.8	2537.6
GLU	57.6	0.0	34.1	94.6	57.6	128.7	186.3	GLU	32	1843.2	0.0	1091.2	3027.2	1843.2	4118.4	5961.6
GLY	40.6	0.0	45.3	0.0	40.6	45.3	85.9	GLY	40	1624.0	0.0	1812.0	0.0	1624.0	1812.0	3436.0
HIS	33.0	82.4	49.7	32.5	115.4	82.2	197.6	HIS	6	198.0	494.4	298.2	195.0	692.4	493.2	1185.6
ILE	156.1	0.0	28.3	0.0	156.1	28.3	184.4	ILE	41	6400.1	0.0	1160.3	0.0	6400.1	1160.3	7560.4
LEU	152.5	0.0	34.0	0.0	152.5	34.0	186.5	LEU	40	6100.0	0.0	1360.0	0.0	6100.0	1360.0	7460.0
LYS	114.5	0.0	33.8	78.2	114.5	112.0	226.5	LYS	35	4007.5	0.0	1183.0	2737.0	4007.5	3920.0	7927.5
MET	167.1	0.0	34.0	0.0	167.1	34.0	201.1	MET	10	1671.0	0.0	340.0	0.0	1671.0	340.0	2011.0
PHE	28.3	157.4	34.0	0.0	185.7	34.0	219.7	PHE	22	622.6	3462.8	748.0	0.0	4085.4	748.0	4833.4
PRO	122.8	0.0	22.5	0.0	122.8	22.5	145.2	PRO	16	1964.0	0.0	359.2	0.0	1964.0	359.2	2323.2
SER	45.0	0.0	83.6	0.0	45.0	83.6	128.6	SER	20	900.0	0.0	1672.0	0.0	900.0	1672.0	2572.0
THR	77.3	0.0	71.7	0.0	77.3	71.7	149.0	THR	36	2782.8	0.0	2581.2	0.0	2782.8	2581.2	5364.0
TRP	29.3	160.8	65.8	0.0	190.1	65.8	255.9	TRP	2	58.6	321.6	131.6	0.0	380.2	131.6	511.8
TYR	28.1	121.5	87.2	0.0	149.6	87.2	236.8	TYR	11	309.1	1336.5	959.2	0.0	1645.6	959.2	2604.8
VAL	134.7	0.0	29.9	0.0	134.7	29.9	164.6	VAL	35	4714.5	0.0	1046.5	0.0	4714.5	1046.5	5761.0
								Totals:	471	41033	5615	22728	9112	46648	31839	78488
flavo																

Table 3-8: Solvent accessible surface areas of the extended polypeptide reference conformation for MerA of *R. marinus*.

"X"	AL area	AR area	PU area	PC area	PHOB area	PHIL area	Total area	"X"	N	AL area	AR area	PU area	PC area	PHOB area	PHIL area	Total area
ALA	79.3	0.0	34.9	0.0	79.3	34.9	114.2	ALA	56	4440.8	0.0	1954.4	0.0	4440.8	1954.4	6395.2
ARG	84.0	0.0	34.1	141.5	84.0	175.6	259.6	ARG	39	3276.0	0.0	1329.9	5518.5	3276.0	6848.4	10124.4
ASN	38.0	0.0	116.4	0.0	38.0	116.4	154.4	ASN	8	304.0	0.0	931.2	0.0	304.0	931.2	1235.2
ASP	38.1	0.0	34.5	79.8	38.1	114.3	152.4	ASP	25	952.5	0.0	862.5	1995.0	952.5	2857.5	3810.0
CYS	106.3	0.0	34.3	0.0	106.3	34.3	140.6	CYS	4	425.2	0.0	137.2	0.0	425.2	137.2	562.4
GLN	55.6	0.0	139.6	0.0	55.6	139.6	195.2	GLN	16	889.6	0.0	2233.6	0.0	889.6	2233.6	3123.2
GLU	57.6	0.0	34.1	94.6	57.6	128.7	186.3	GLU	34	1958.4	0.0	1159.4	3216.4	1958.4	4375.8	6334.2
GLY	40.6	0.0	45.3	0.0	40.6	45.3	85.9	GLY	46	1867.6	0.0	2083.8	0.0	1867.6	2083.8	3951.4
HIS	33.0	82.4	49.7	32.5	115.4	82.2	197.6	HIS	10	330.0	824.0	497.0	325.0	1154.0	822.0	1976.0
ILE	156.1	0.0	28.3	0.0	156.1	28.3	184.4	ILE	22	3434.2	0.0	622.6	0.0	3434.2	622.6	4056.8
LEU	152.5	0.0	34.0	0.0	152.5	34.0	186.5	LEU	59	8997.5	0.0	2006.0	0.0	8997.5	2006.0	11003.5
LYS	114.5	0.0	33.8	78.2	114.5	112.0	226.5	LYS	5	572.5	0.0	169.0	391.0	572.5	560.0	1132.5
MET	167.1	0.0	34.0	0.0	167.1	34.0	201.1	MET	2	334.2	0.0	68.0	0.0	334.2	68.0	402.2
PHE	28.3	157.4	34.0	0.0	185.7	34.0	219.7	PHE	12	339.6	1888.8	408.0	0.0	2228.4	408.0	2636.4
PRO	122.8	0.0	22.5	0.0	122.8	22.5	145.2	PRO	23	2823.3	0.0	516.4	0.0	2823.3	516.4	3339.6
SER	45.0	0.0	83.6	0.0	45.0	83.6	128.6	SER	18	810.0	0.0	1504.8	0.0	810.0	1504.8	2314.8
THR	77.3	0.0	71.7	0.0	77.3	71.7	149.0	THR	29	2241.7	0.0	2079.3	0.0	2241.7	2079.3	4321.0
TRP	29.3	160.8	65.8	0.0	190.1	65.8	255.9	TRP	3	87.9	482.4	197.4	0.0	570.3	197.4	767.7
TYR	28.1	121.5	87.2	0.0	149.6	87.2	236.8	TYR	13	365.3	1579.5	1133.6	0.0	1944.8	1133.6	3078.4
VAL	134.7	0.0	29.9	0.0	134.7	29.9	164.6	VAL	43	5792.1	0.0	1285.7	0.0	5792.1	1285.7	7077.8
								Totals:	467	40242	4775	21180	11446	45017	32626	77643
rhodo																

Table 3-9: Solvent Accessible Surface Areas by Type of Atom ($Å^2$).

	Tn*501*	SOK62	*R. marinus*
Aliphatic area	9995.1	10944.1	10365.5
Aromatic area	975.9	1244.2	1036.9
Polar uncharged area	4696.7	5543.5	4442.2
Polar charged area	4817.6	4374.3	5128.9
Total hydrophobic area (aliph + arom)	10971	12188.3	11402.4
Total polar area (uncharged + charged)	9514.3	9917.8	9571.1
Overall total accessible surface area	20485.3	22106.1	20973.5

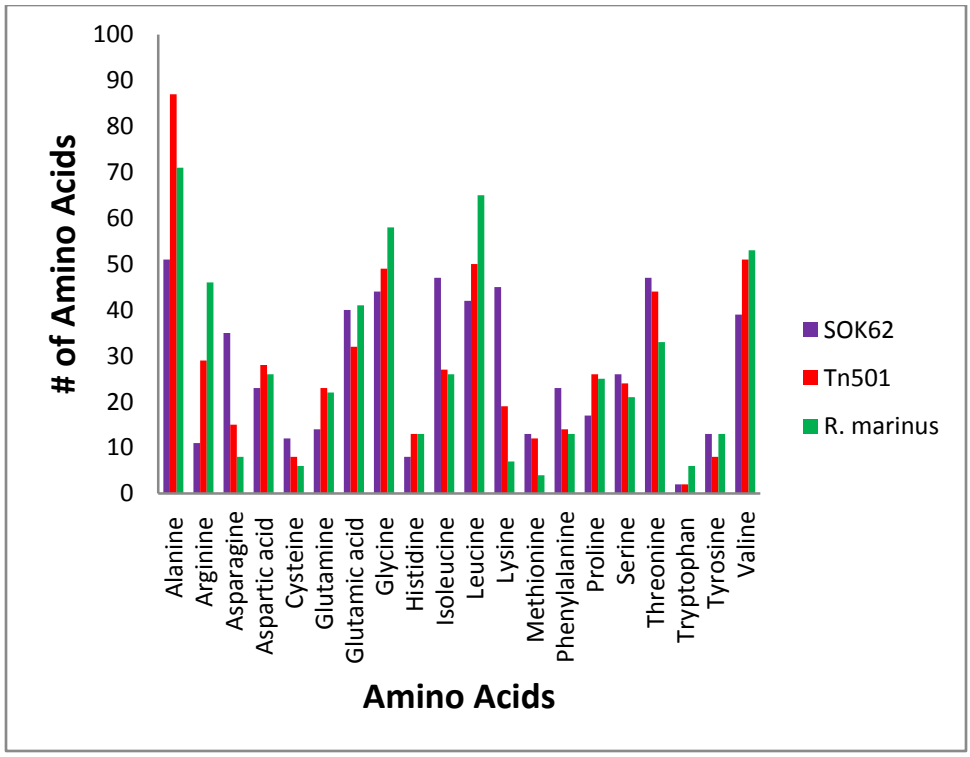

Figure 3-8: Comparison of number of residues among the 3 MerA sequences.

3.4 Conclusion/Discussion

Comparison of the 3 models indicates that first, SOK62 has a larger number of α helices or loops [37] and fewer β sheets (Table 3-5) and also more polar residues (Table 3-4), suggesting higher flexibility, and therefore adaptation to activity at lower temperature than MerA of *R. marinus*. Second, SOK62 MerA contains 3 additional Cys pairs (Figure 3-9) whose function will be determined later.

In general, cysteines have a functional role in several processes such as nucleophilic and redox catalysis, allosteric regulation, metal binding, etc. [38]. In the presence of light, cysteine nucleophilicly attacks the flavin ring of FAD molecules (an FAD exists around the active site of MerA, which consists of 13 conserved residues:

GGTCVNVGCVPSK). Covalent binding to flavin is important to the active site of MerA, and it could be achieved by three extra cysteine pairs of SOK62. At low temperatures, the molecular motion is slower and, a higher number of cysteine pairs can compensate the transport of mercury to the active site.

SOK62 has three extra pairs including Cys44 and Cys46, Cys78 and Cys79, and Cys331 and Cys333 (Figure 3-9). The extra cysteine pairs have been found in several MerA sequences. The **first** cysteine pair (Cys44 and Cys46) is found in *Belliellabaltica* DSM 15883, *Flavobacterium frigoris* PS1, *Sphingobacterium spiritivorum* ATCC 33300, *Chryseobacterium gleum* ATCC 35910, and *Cyclobacterium marinum* DSM 745. The **second** cysteine pair (Cys78 and Cys79) is found in *Oligotropha carboxidovorans* OM5, *Thalassospira profundimaris* WP0211, *alpha proteobacterium* BAL199, *Afipia clevelandensis* ATCC 49720, *Sphingopyxis alaskensis* RB2256, *and Roseo varius* sp. 217, *Rhizobium sp*., *Oceanico labatsensis* HTCC2597, *Maritimi bacteralkaliphilus* HTCC2654, *Acidiphilium multivorum* AIU301, and *Sphingobium* sp.SYK-6. The **third** cysteine pair is found in *Belliellabaltica* DSM 15883, *Flavobacterium frigoris* PS1, *Sphingobacterium spiritivorum* ATCC 33300, *Chryseo bacteriumgleum* ATCC 35910, *Cyclobacterium marinum* DSM 7, *and Galbibacter*. sp. ck-I2-15, and *Tenacibaculum discolor* (Table 3-10). The conclusion is that the 1st and 3rd pairs are only found in bacteroidetes and pair 2 only in SOK62 and the Alphaproteobacteria.

Table 3-10: Extra cysteine pairs found in *Bacteroidetes* and *proteobacteria.*

#	Name	Taxonomy	Optimum growth temperature	Extra Cys pair
1	*Belliellabaltica*	Bacteroidetes	25 °C	1st,3rd
2	*Flavobacterium frigoris*	Bacteroidetes	psychrophile	1st,3rd
3	*Sphingobacterium spiritivorum* ATCC 33300	Bacteroidetes	26.0°C	1st,3rd
4	*Chryseo bacteriumgleum* ATCC 35910	Bacteroidetes	30.0°C	1st,3rd
5	*Cyclo bacterium marinum* DSM 745	Bacteroidetes	20-25C	1st,3rd
6	*Oligo trophacarboxidovorans*	Alphaproteobacteria	Mesophile	2nd
7	*Thalassospira* profundimaris	Alphaproteobacteria	22˚C)	2nd
8	*Afipia clevelandensis*	Alphaproteobacteria	30.0°C	2nd
9	*Sphingopyxis alaskensis*	Alphaproteobacteria	24 °C	2nd
10	*Roseovarius* sp. 217	Alphaproteobacteria	20 to 25°C	2nd
11	*Oceani colabatsensis*	Alphaproteobacteria	28–30 °C	2nd
12	*Maritimi bacteralkaliphilus*	Alphaproteobacteria	30 °C	2nd
13	*Acidiphilium multivorum* AIU301	Alphaproteobacteria	Mesophile	2nd
14	Sphingobium sp. SYK-6	Alphaproteobacteria	30°C	2nd
15	Galbibacter .sp	Bacteroidetes	at 25–30	3rd
16	*Tenacibaculum discolor*	Bacteroidetes	25–30 °C	3rd

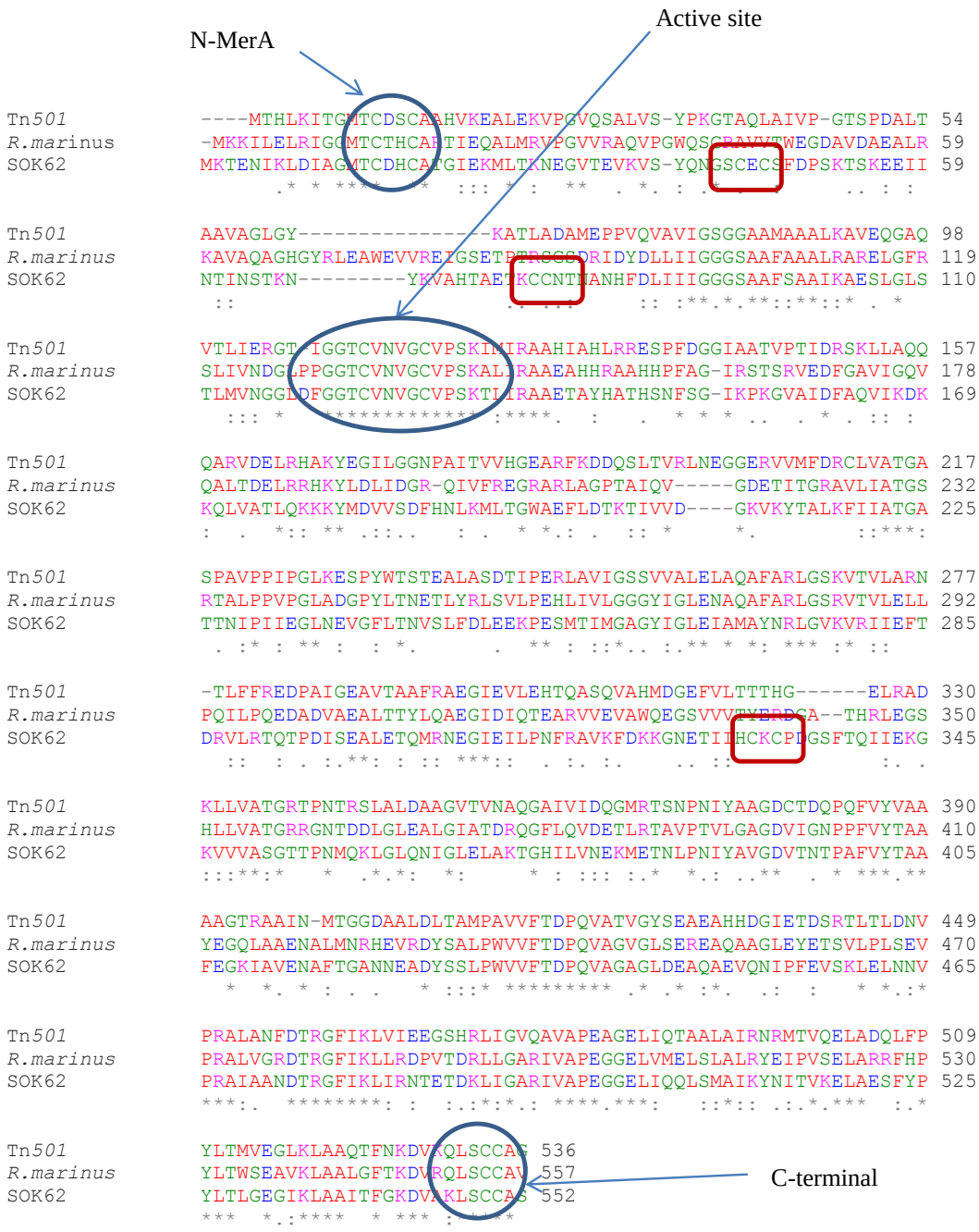

Figure 3-9: Multiple alignment of the three MerA. Circles highlight conserved functional motifs from top to bottom: N-merA metal binding motif, redox active site, and carboxyl terminal vicinal cysteine pair. Red boxes indicate extra cysteine pairs found only in SOK62.

The functions of the extra cysteine pairs could be the following:

1. At low temperatures, the molecular motion is slower, and a higher number of Cys pairs can compensate, facilitating the transport of mercury to the active site (adaptation in cold microorganism [30]).
2. Playing a role to stabilize proteins against thermal denaturation (thermal stability) [39].
3. Increase in the stability and rigidity (disulfide bonds) [40]and decrease in the flexibility of the protein [40].
4. MerA works as a homodimer [41]**(**shown in Figure 3-10**),** and there is possibility that the extra cysteines have a role in the interaction between the two monomers.

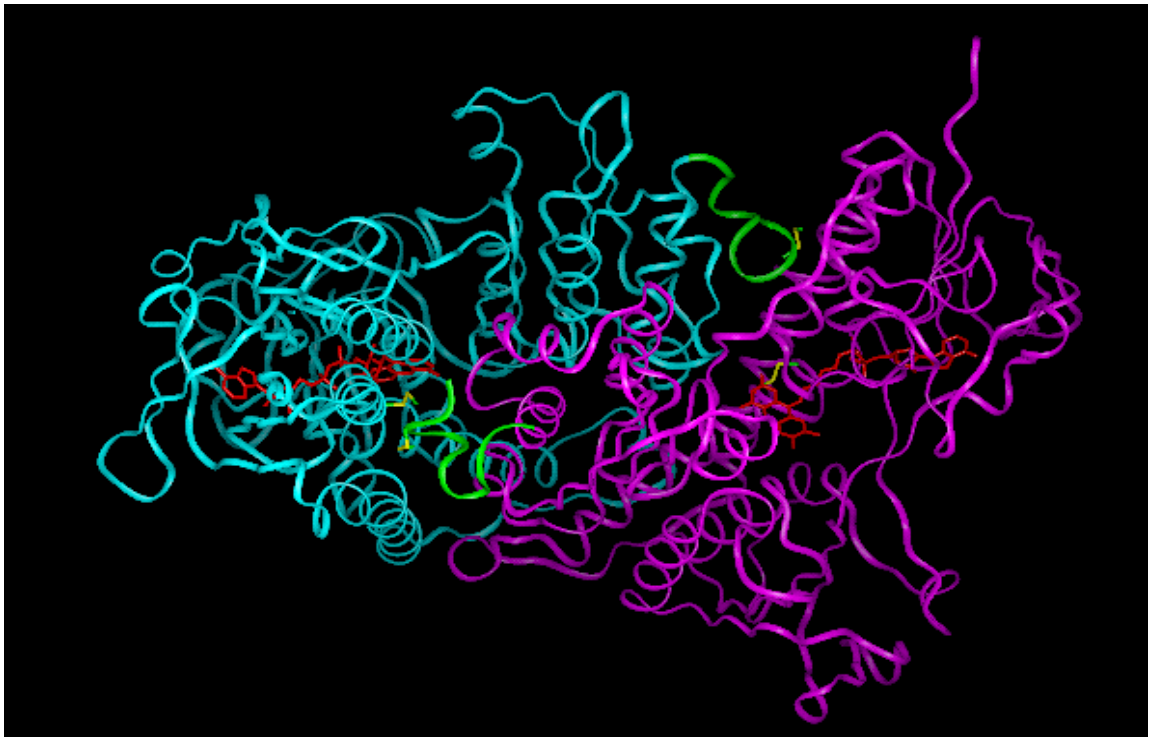

Figure 3-10: MerA as a homodimer (shown here without N-merA): Blue and purple is core MerA; green is the carboxyl terminal; red illustrates the bound FAD; yellow highlight cysteine residues.

Future Work

It will be beneficial to perform further analysis of the models such as checking the positions of extra cysteine pairs and their distance to active site or other mercury binding domain. In addition, it is important to check where in the secondary structure they are located, *i.e.*, in α-helices, β-sheets, or in the loops. Finally, it is helpful to induce Site-directed mutagenesis in order to investigate the structure and molecular activity of MerA, to find the critical residues for enzyme activity, for example, by replacing these extra cysteines of SOK62 with other residues, using site directed mutagenesis and then to run the merA assay to compare the activity of MerA containing cysteine with mutated MerA.

References

[1] R. Allen, Y. Tu, M. Nevarez, A. Bobbs, J. Friesen, J. Lorsch, J. McCauley, J. Voet and N. Hamlett, "The mercury resistance (mer) operon in a marine gliding flavobacterium, Tenacibaculum discolor 9A5," *J.Fems Microbiol Ecol,* vol. 83, pp. 135-148, 2013.

[2] B. Fox and C. Walsh, "Purification and characterization of a transposon-encoded flavoprotein containing an oxidation-reduction-active disulfide," *J.Biological Chemistry,* vol. 257, pp. 2498-2503, 1981.

[3] G. Feller and C. Gerday, "Psychrophilic enzymes: hot topics in cold adaptation," *J.Nature Reviews Microbiology,* vol. 1, pp. 200-208, 2003.

[4] T. Barkay, K. Kritee, E. Boyd and G. Geesey, "A thermophilic bacterial origin and subsequent constraints by redox, light and salinity on the evolution of the microbial mercuric reductase," *J.Environmental Microbiology,* vol. 12, pp. 2904-2917, 2010.

[5] C. Lin, N. Yee and T. Barkay, "Microbial Transformations in the Mercury Cycle," in *Environmental Chemistry and Toxicology of Mercury,* Hoboken,NJ, John Wiley & Sons, Inc., 2012, pp. 155-191.

[6] E. S. Boyd and T. Barkay, "The Mercury Resistance Operon: From an Origin in a Geothermal Environment to an Efficient Detoxification Machine," *J.Front Microbiol,* vol. 3, pp. 1-13, 2012.

[7] T. Barkay, S. M. Miller and A. Summers, "Bacterial mercury resistance from atoms to ecosystems," *J.Fems Microbiology Reviews,* vol. 27, pp. 355-384, 2003.

[8] H. Griffin, T. Foster, S. Silver and T. Misra, "Cloning and DNA sequence of the mercuric and organomercurial resistance determinants of plasmid pDU1358," *J.Biochemistry,* vol. 84, pp. 3112-3116, 1987.

[9] N. L. Brown, S. J. Ford, R. D. Pridmore and D. Fritzinger, "Nucleotide sequence of a gene from the Pseudomonas transposon Tn501 encoding mercuric reductase," *J.Biochemistry,* vol. 22, pp. 4089-95, 1983.

[10] T. Misra, N. Brown, L. Haberstroh, A. Schmidt, D. Goddette and S. Silver, "Mercuric reductase structural genes from plasmid R100 and transposon Tn501: functional domains of the enzyme," *J.Gene,* vol. 34, pp. 253-262, 1985.

[11] B. Hong, R. Nauss, I. Harwood and S. Miller, "Direct Measurement of Hg(II) Removal from Organomercurial Lyase (MerB) by Tryptophan Fluorescence: NmerA Domain of Co-evolved γ -Proteobacterial Mercuric Ion Reductase (MerA) Is More Efficient than MerA Catalytic Core or Glutathione," *J.Biochemistry,* vol. 49, pp. 8187-8196, 2010.

[12] S. Miller, M. Moore, V. Massey, C. J. Williams, M. Distefano, D. Ballou and C.

Walsh, "Evidence for the participation of Cys558 and Cys559 at the active site of mercuric reductase," *J.Biochemistry*, vol. 28, pp. 1194-205, 1989.

[13] A. Johs, I. Harwood, J. Parks, R. Nauss, J. Smith, L. Liang and S. Miller, "Structural characterization of interamolecular Hg2+ transfer between flexibly linked domains of Mercuric Ion Reductase," *J.Molecular Biology*, vol. 413, pp. 639-656, 2011.

[14] Z. Freedman, C. Zhua and T. Barkay, "Mercury Resistance and Mercuric Reductase Activities and Expression among Chemotrophic Thermophilic Aquificae," *J.Appl. Environ. Microbiol*, vol. 78, pp. 6568-6575, 2012.

[15] C. Vetriani, Y. Chew, S. Miller, J. Yagi, J. Coombs, R. Lutz and T. Barkay, "Mercury Adaptation among Bacteria from a Deep-Sea Hydrothermal Vent," *J.Applied and Environmental Microbiology*, vol. 71, pp. 220-226, 2005.

[16] A. J. Poulain, S. M. Chadhain, P. A. Ariya, M. Amyot, E. Garcia, P. G. C. Campbell, G. Z. Zylstra and T. Barkay, "Potential for Mercury Reduction by Microbes in the High Arctic," *J.Applied and Environmental Microbiology*, vol. 73, pp. 2230-2238., 2007.

[17] A. Møller, T. Barkay, W. Al-Soud, S. Sørensen, H. Skov and N. Kroer, "Diversityand characterization of mercury-resistant bacteria in snow,freshwater and sea-ice brine from the High Arctic," *J.Fems Microbiol Ecol*, vol. 75, pp. 390-401, 2011.

[18] A. Alfredsson, K. Kristjansson, S. Hjörleifsdottir and K. Stetter, "Rhodothermus marinus, gen. nov., sp. nov., a Thermophilic, Halophilic Bacterium from Submarine Hot Springs in Iceland," *J.General MicrobioIogy*, vol. 134, pp. 299-306, 1988.

[19] G. J. Vanderheiden, A. C. Fairchild and G. R. Jago, "Construction of a Laboratory Press for Use with the French Pressure Cell," *J.Applied Microbiology*, vol. 19, pp. 875-877, May 1970.

[20] W. Ying, "NAD(+)/ NADH and NADP(+)/NADPH in cellular functions and cell death: Regulation and biological consequences," *J.Antioxid Redox Signal*, vol. 10, pp. 179-206, 2008.

[21] J. Parker and N. Bloom, "Preservation and storage techniques for low-level aqueous mercury speciation," *J.Science of the Total Environment*, vol. 337, pp. 253-263, 2005.

[22] M. M. Bradford, "A rapid and sensitive method for the quantitation of microgram quantities of protein utilizing the principle of protein-dye binding.," *J.Anal Biochem*, vol. 72, pp. 248-54, 1976.

[23] A. Dereeper, V. Guignon, G. Blanc, S. Audic, S. Buffet, F. Chevenet, J. F. Dufayard, S. Guindon, V. Lefort, M. Lescot, J. M. Claverie and O. Gascuel, "Phylogeny.fr: robust phylogenetic analysis for the non-specialist," *J.Nucleic Acids Research*, vol. 36, pp. 465-469, 2008.

[24] A. Dereeper, S. Audic, J. Claverie and G. Blanc, "BLAST-EXPLORER helps you building datasets for phylogenetic analysis," *J.BMC Evolutionary Biology,* vol. 10, pp. 1-6, 2010.

[25] T. Barkay and I. W. Döbler, "Microbial Transformations of Mercury: Potentials, Challenges, and Achievements in Controlling Mercury Toxicity in the Environment," *J.Advances in Applied Microbiology,* vol. 57, pp. 1-52, 2005.

[26] Y. Wang, Z. Freedman, P. Lu-Irving, R. Kaletsky and T. Barkay, "An initial characterization of the mercury resistance (mer) system of the thermophilic bacterium Thermus thermophilus HB27," *J.Fems Microbiol Ecology,* vol. 67, pp. 118-129, 2009.

[27] S. E. Lindberg, S. Brooks, C. J. Lin, K. J. Scott, M. S. Landis, R. K. Stevens, M. Goodsite and A. Richter, "Dynamic Oxidation of Gaseous Mercury in the Arctic Troposphere at Polar Sunrise," *J.Environ. Sci. Technol,* vol. 36, pp. 1245-1256, 2002.

[28] A. Sayed, M. Ghazy, A. Ferreira, J. Setubal, F. Chambergo, A. Ouf, M. Adel, A. Dawe, J. Archer, V. Bajic, R. Siam and H. El-Dorry, "A novel mercuric reductase from the unique deep brine environment of Atlantis II in the Red Sea," *J. Biological Chemistry,* vol. 17, pp. 1675-1687, 2014.

[29] R. P. R. Metpally and B. V. B. Reddy, "Comparative proteome analysis of psychrophilic versus mesophilic bacterial species: Insights into the molecular basis of cold adaptation of proteins," *J.BMC Genomics,* vol. 10, pp. 1-10, 2009.

[30] A. Szilágyi and P. Závodszky, "Structural differences between mesophilic, moderately thermophilic and extremely thermophilic protein subunits: results of a comprehensive survey," *J.Structure,* vol. 15, pp. 493-504, 2000.

[31] C. Vieille and G. Zeikus, "Hyperthermophilic Enzymes: Sources, Uses, and Molecular Mechanisms for Thermostability," *J.Microbiology and Molecular Biology Reviews,* vol. 65, pp. 1-43, 2001.

[32] S. Amico, T. Collins, J. Marx, G. Feller and C. Gerday, "Psychrophilic microorganisms: challenges for life," *J.EMBO Reports,* vol. 7, pp. 385-389, 2006.

[33] R. Ledwidge, B. Patel, A. Dong, D. Fiedler, M. Falkowski, J. Zelikova, A. Summers, E. Pai and S. Miller, "NmerA, the metal binding domain of mercuric ion reductase, removes Hg2+ from proteins, delivers it to the catalytic core, and protects cells under glutathione-depleted conditions.," *J.American Chemical Society,* vol. 44, pp. 11402-11416, 2005.

[34] B. Lee and F. M. Richards, "The Interpretation of Protein Structures: Estimation of Static Accessibility," *J. Molecular Biology,* vol. 55, pp. 379-490, 1971.

[35] T. Kajander, A. L. Cortajarena, E. R. G. Main, S. G. J. Mochrie and L. Regan, "A New Folding Paradigm for Repeat Proteins," *J. American Chemical Society,* vol. 127, no. 29, pp. 10188-10190, 2005.

[36] F. M. Richards, "The Interpretation of Protein Structures: Total Volume, Group Volume Distributions and Packing Density," *J. Molecular Biology*, vol. 82, no. 1, pp. 1-14, 1974.

[37] E. Narinx, C. Baise and C. Gerday, "Subtilisin from psychrophilic antarctic bacteria: characterization and site-directed mutagenesis of residues possibly involved in the adaptation to cold," *J.Protein Engineering*, vol. 10, pp. 1271-1279, 1997.

[38] N. Pace and E. Weerapana, "Diverse Functional Roles of Reactive Cysteines," *J.ACSC Biology*, vol. 8, pp. 283-296, 2013.

[39] M. Beeby, B. D. O'Connor, C. Ryttersgaard, D. R. Boutz, L. J. Perry and T. O. Yeates, "The Genomics of Disulfide Bonding and Protein Stabilization in Thermophiles," *J.Plos Biology*, vol. 3, pp. 1549-1558, 2005.

[40] S. Amico, C. Gerday and G. Feller, "Dual Effects of an Extra Disulfide Bond on the Activity and Stability of a Cold-adapted alpha-Amylase," *J.Biological Chemistry*, vol. 277, pp. 46110-46115, 2002.

[41] D. Rennex, R. Cummings, M. Pickett, C. Walsh and M. Bradley, "Role of Tyrosine Residues in Hg(II) Detoxification by Mercuric Reductase from," *J.Biochemistry*, vol. 32, pp. 7475-7478, 1993.